DEPARTMENT OF MECHANICAL ENGINEERING & MECHANICS
COLLEGE OF ENGINEERING & TECHNOLOGY
OLD DOMINION UNIVERSITY
NORFOLK, VIRGINIA 23529

DYNAMICS AND CONTROL OF A FIVE DEGREE-OF-FREEDOM MAGNETIC SUSPENSION SYSTEM

By

Anwar Mohammed Haj, Graduate Research Assistant

Principal Investigator: Colin P. Britcher

Progress Report
For the period November 1, 1991 to April 30, 1992

Prepared for
National Aeronautics and Space Administration
Langley Research Center
Hampton, VA 23665

Under
Research Grant NAG-1-1056
Nelson J. Groom, Technical Monitor
GCD-Spacecraft Controls Branch

Submitted by the
Old Dominion University Research Foundation
P.O. Box 6369
Norfolk, Virginia 23508-0369

June 1992

DYNAMICS AND CONTROL OF A FIVE DEGREE-OF-FREEDOM MAGNETIC SUSPENSION SYSTEM

ABSTRACT

By

Anwar Mohammed Haj[1]

Principal Investigator: Colin P. Britcher[2]

A large-gap magnetic suspension system with five degrees-of-freedom is presented. The system is multi-input multi-output with coupling between degrees-of-freedom. Simulation was performed on this multi degree-of-freedom system in order to control each degree-of-freedom separately. Two types of controllers are considered by adding white noise to a single degree-of-freedom system in order to test their behavior and determine which is the best choice for the system. The responses of the system are produced in continuous and discrete time where a sample interval and delay time was introduced. Using these responses, a comparison between each degree-of-freedom was made and the maximum value of the delay time was determined.

---

[1]Graduate Research Assistant, Department of Mechanical Engineering and Mechanics, Old Dominion University, Norfolk, VA 23529.

[2]Assistant Professor, Department of Mechanical Engineering and Mechanics, Old Dominion University, Norfolk, Va 23529.

ACKNOWLEDGEMENTS

This is a thesis being submitted in lieu of a progress report for the research project entitled "Large Angle Magnetic Suspension Test Fixture" for the period November 1, 1991 through April 30, 1992. This work was partially supported by the NASA Langley Research Center through research grant NAG-1-1056 and monitored by Nelson J. Groom, of the GCD, Spacecraft Controls Branch, NASA Langley Research Center, Mail Stop 161.

TABLE OF CONTENTS

LIST OF SYMBOLS

a, b	constants
B	flux density (Tesla)
C	damping coefficient
$\frac{d}{dt}$	derivative with respect to time
f	external input force
F	force (N)
F_A	attraction force
F_g	gravitational force
F_D	damping force
$\bar{F}$	force on core (model) in core's coordinates
$\bar{F}_m$	electromagnet forces
$\bar{F}_d$	external disturbance forces
g	acceleration due to gravity (m/s^2)
$\bar{H}$	momentum of the model
i	current (Amps)
i_0	equilibrium current
ΔI	S-domain small change in current
I	product of inertia
K	gain
K_B	matrix representing the values of B
K_c	coil constant
K_i	linearization constant

K_x	linearization constant
L	inductance (H)
m	mass (kg)
m_c	the core (model) mass
M	core (model) magnetization (A/m)
R	resistance (Ω)
S	laplace variable
t	time (seconds)
$\bar{T}$	total torque about core (model) center of mass
$\bar{T}_m$	electromagnets torque
$\bar{T}_d$	external disturbance torques
u	input
V	voltage
$\bar{V}$	core (model) velocity
V_0	equilibrium voltage
V_D	power supply input
ΔV	S-domain small change in voltage
V, V'	output from controller
x	position, separation distance (m)
$\dot{x}$	first derivative of position, velocity
$\ddot{x}$	second derivative of position, acceleration
ΔX	S-domain small change in position
y	state space output
δ	small variation in parameter

σ	variance
$\bar{\Omega}$	angular velocity (rad/sec)
μ	permeability of material in free space, equal 4π x 10^{-7} (Henrys/m)
Γ	standard deviation
$\frac{\partial}{\partial x}$	partial derivative with respect to x
$\frac{\partial}{\partial i}$	partial derivative with respect to i

LIST OF FIGURES

Figure **Page**

LIST OF TABLES

NOMENCLATURE

D P A	Dual Phase Advance
MIT	Massachusetts Institute of Technology
MSBS	Magnetic Suspension and Balance System
LGMSS	Large-Gap Magnetic Suspension System
NAL	National Aerospace Laboratory, Japan
NASA	National Aeronautics and Space Administration, United States
ONERA	Office National d'Etudes et de Recherches Aèrospatiales, France
TsAGI	The Central Aero-Hydrodynamics Institute, Soviet Union
P D	Proportional Derivative
P I D	Proportional Integral Derivative
SISO	Single Input Single Output
UVa	University of Virginia

CHAPTER 1

INTRODUCTION

An actively stabilized magnetic suspension system was first used at the University of Virginia, USA, in 1937 (Ref. 1). Such systems are now being used in a variety of applications including world-wide investigation for advanced ground transportation schemes and also for application in contactless bearings for high and very low speeds. Additional applications include rotors of high speed centrifuges required in the fields of biology and medicine; testing bursting speeds of spheres such as ball bearings; testing adhesion of metal films; turbomolecular pumps for high vacuums free of bearings requiring lubricants. The same principle has been used to suspend aircraft models in wind tunnels which helps the investigation of more subtle aerodynamic details and improves techniques for studying aero-vehicle stability.

The researchers at the Office National d'Etudes et de Recherches Aèrospatiales (ONERA), France were first to achieve magnetic suspension of models in a wind tunnel in 1957 (Ref. 2). The ONERA system controlled models in five degrees-of-freedom in test sections up to 30 cm in diameter. So far it is believed that about 17 wind tunnel magnetic suspension systems have been built since then, with six currently in operation (Ref. 3,4). Of these six wind tunnels, two are at NASA Langley Research Center in the USA. The others are at Oxford University and the University of Southampton in England, the National Aerospace Laboratory (NAL) in Japan, and the Central Aero-Hydrodynamics Institute (TsAGI) in the Soviet Union. Table 1.1 gives the detailed listings of those wind tunnel systems.

Most magnetic suspension and balance systems require the use of controlled dc electromagnets acting on suspended body composed of a ferromagnetic material. Using this approach, a feedback controller is required for the stabilization of the position and attitude of the

suspended body. Other approaches generally cannot generate high damping, especially with large air-gaps. The following is a list of these systems (Ref. 14)

1) Levitation using forces of repulsion between permanent magnets. Stable suspension or levitation is impossible with a system of permanent magnets (or fixed current electromagnets) unless part of the system contains either diamagnetic material or a superconductor. Developments in fabricating permanent magnet material have raised interest in the idea of using such magnets. The most common application of such magnets is in the suspension of shafts or spindles.

2) Levitation using forces of repulsion between diamagnetic materials. Levitation can be achieved in static magnetic fields by employing diamagnetic material. However, even the two materials which exhibit the most pronounced diamagnetic properties, i.e. bismuth and graphite, are so weakly diamagnetic that only small pieces can be levitated.

3) Levitation using superconducting magnets. The superconducting state is indicated by the complete absence of electrical resistance, and once initiated a current will continue to flow without the presence of a voltage source in the circuit. One of the primary applications is an electrodynamically levitated vehicle lifted and guided by repulsion forces between superconducting magnets on the vehicle and secondary circuits on the track (eddy currents if the track circuits are passive). The stiffness and damping of the suspension are low, and the vehicle must be in motion in order to generate lift. Therefore, there is a minimum velocity which must be exceeded before the vehicle becomes levitated. Some of the problems and drawbacks that remain unsolved are that in addition to the aerodynamic drag on such vehicles there is an eddy current drag which is large at low speeds. More recently, however, due to developments in linear induction motors, particularly of the transverse flux type, it has been claimed that such machines might be used for combined levitation and

propulsion of high speed vehicles.

4) Suspension using a tuned LCR circuit and the electromagnetic force of attraction between two plates. The variation of the inductance of an electromagnet in the proximity of a ferromagnetic object, depending on the separation between the two, is utilized in this method to regulate the current and hence the attraction force. This is achieved by incorporating the electromagnet within an LCR circuit tuned in such a way that when the object to be suspended moves away from the electromagnet the circuit tends to become resonant, thus increasing the current and hence the force acting on it. The main disadvantages stem from the fact that at the equilibrium point the circuit is predominantly inductive and hence the reactive power input is rather large. Also the iron structure including the object to be suspended must be laminated to reduce eddy current losses.

There is a wide range of applications associated with large-gap magnetic suspension technology, including microgravity and vibration isolation systems, magnetically suspended pointing mounts, large-angle magnetic suspension systems for advanced actuators, wind tunnel magnetic suspension systems, and remote manipulation/control/positioning of objects in space.

The Large-Gap Magnetic Suspension System (LGMSS) is a hypothetical design for a ground-based experiment that could be used to investigate the technology issues associated with magnetic suspension systems at large gaps, accurate suspended element control at large gaps, and accurate position sensing at large gaps.

The uncontrolled and unknown aerodynamic loads on model in wind tunnel have to be magnetically opposed by the MSBS while the absence of these loads in the LGMSS causes a reduction in the magnetic field intensity and the dynamic force and moment requirements. A model in a MSBS is never stationary, since the systems are open-loop unstable and rely on

position and attitude error feedback for stabilization.

The two controllers that are most commonly used with the magnetic suspension systems are the phase-advance and proportional-integral-derivative (PID) controllers.

This report will concentrate on the development of a simulation of the five degree-of-freedom Large-Gap Magnetic Suspension System. The behavior of the system is observed when each degree-of-freedom is activated and the coupling of certain degrees-of-freedom is observed. For this simulation, continuous-time step responses and discrete-time step responses including the effect of time delay were used to monitor the behavior of the system.

This report will also examine the effect of random noise when added to the single-degree-of-freedom system with either the Phase Advance controller or the PID controller to indicate which controller is best suited for this system.

Organization	Degrees of Freedom	Size, cm	Controller
NAL	5	10 x 10	digital
NASA Langley	5	26.7 x 31.8	digital
NASA Langley	5/6	15 oct.	analog
Oxford University	3	12 x 12	analog
TsAGI	5	40 x 60	analog
University of Southampton	5/6	18 oct.	digital

Table 1.1 Wind Tunnel Magnetic Suspension and Balance Systems.

CHAPTER 2

BACKGROUND

2.1 Magnetic Suspension and Balance System (MSBS)

Until recently, the development of multi-degree-of-freedom magnetic suspension systems has been hindered by the limited flexibility of control systems. Magnetic suspension devices of the type under consideration can be made stable with a feedback control system (Fig. 2.1). In order to achieve stable suspension it is necessary to devise means of regulating the current in one or more electromagnets using position feedback of the object to be suspended. Further, it can be shown that feedback of some form of rate information is necessary. In magnetic suspension applications this cannot usually be achieved by direct sensing. Instead, rate information is synthesized in the controller by differentiation of the position data (PID controller) or by a DPA controller (usually referred to as "lead"). Assuming that the suspended object position is the controlled variable, the "controller" can be placed ahead of a position demand input (in the feedback path, H(s) in or after this input (feedforward path, G(s)) (Fig. 1). Closed loop stability is the same in both cases, whereas the response to demanded changes in object position is quite different. Position error integrators are often added and located in the forward path.

Two important variables of relevance to the digital controller are the sample interval and the time delay. These quantities are not necessarily equal but will be regarded as such in analysis. Complex multi-degree-of-freedom systems tend to force these two quantities to be roughly equal since all the degrees-of-freedom are sampled together to produce input to the controller. Once all the degrees-of-freedom are processed and command output, the sampling procedure starts again without allowing any further delay time.

2.2 Large-Gap Magnetic Suspension System (LGMSS)

The Large-Gap Magnetic Suspension System is composed of five electromagnets and a suspended ferromagnetic object. The suspended ferromagnetic object contains a core which is a cylinder composed of permanent magnet material, and the magnetic actuators are air core electromagnets mounted in a planar array. The core is suspended or levitated by repulsive forces produced by the five electromagnets which are mounted horizontally. The permanent magnet material provides the needed magnetic field which interacts with the fields of the suspension electromagnets to produce suspension and positioning forces and torques.

The LGMSS, which has an air-gap of about 1 meter, provides five degree-of-freedom control where the suspended element is a cylinder composed of permanent magnet material. In the LGMSS (Fig. 2), the model's own weight is the principal force acting on the levitated model, in addition to some other loads that may be anticipated. The model's spatial position and orientation are to be maintained to high accuracy, with very small allowable undemanded motion around any particular location. However, the position and attitude must be variable under operator control, preferably over a wide range. The rate of movement from one position or attitude to another may be slow.

The uncontrolled degree of freedom is rotation about the long axis of the suspended cylinder. The analytical model consists of an open-loop representation of the suspension system with electromagnet currents as inputs and displacements and rates in inertial coordinates as outputs.

The proper description of the power supply is actually a power amplifier, since controlled currents must be supplied to the load electromagnet by varying the amplifier output voltage.

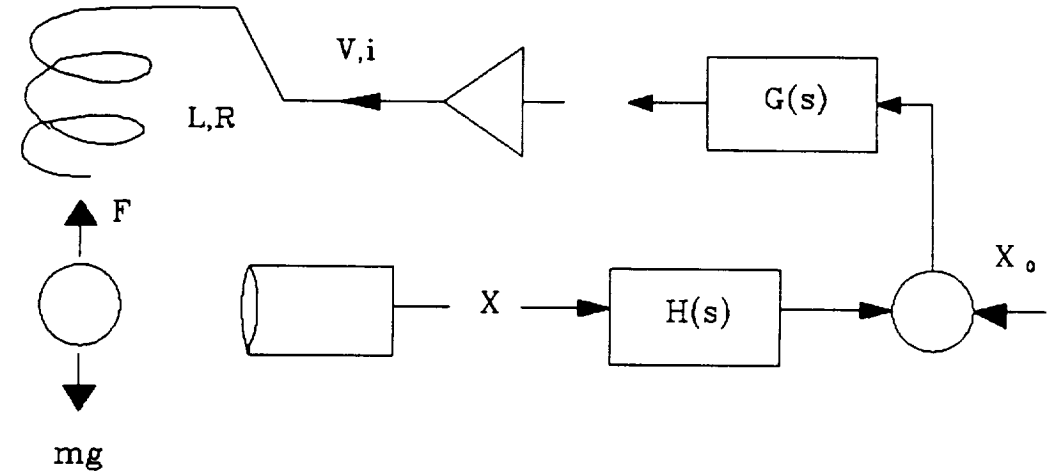

Figure 1 Magnetic suspension controller arrangement.

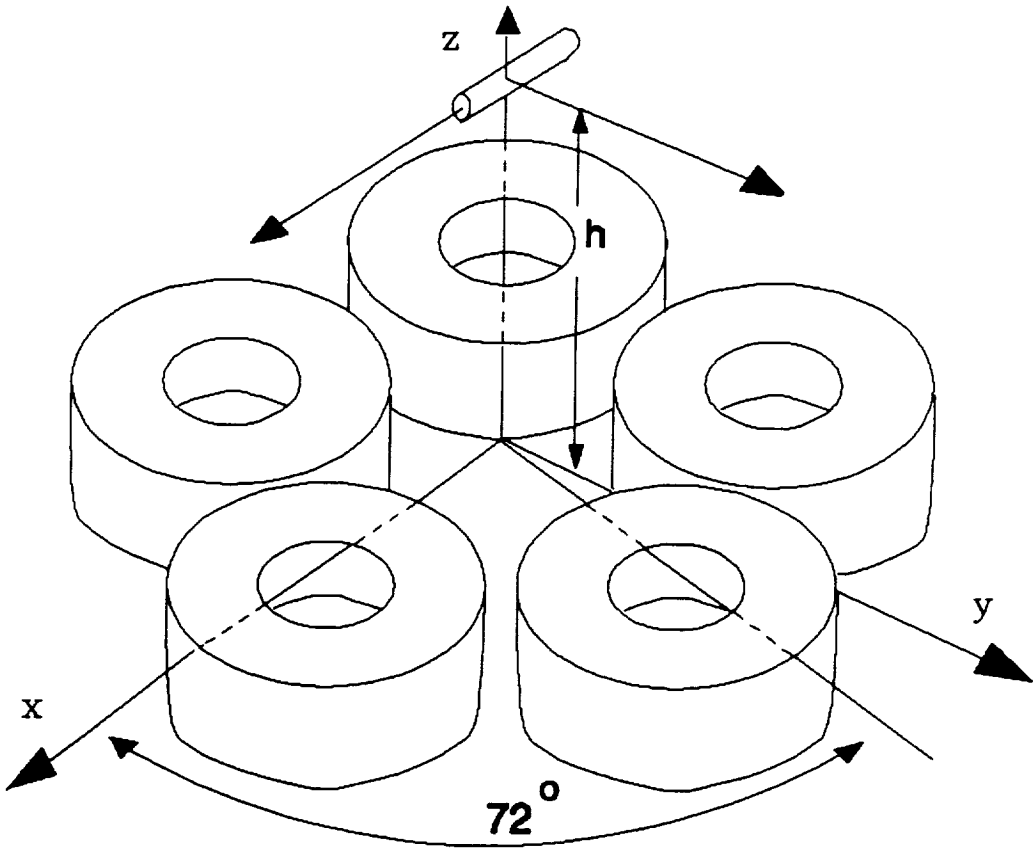

Figure 2 Schematic of five coil Large-Gap Magnetic Suspension System.

CHAPTER 3

GOVERNING EQUATIONS

3.1 Single Degree-of-Freedom System (MSBS)

Equations for a one degree-of-freedom magnetic suspension system (Ref. 6) are derived starting with Newton's second law of motion. The resulting equations are converted to the S-domain using Laplace transforms and then the state-space form of these equations is obtained. The equation of motion for the body is

$$m\ddot{x} = F_g - F_A(x,i) - F_D + f \tag{3.1.1}$$

where F_g is the weight of the body, F_A is the magnetic force exerted on the body by the electromagnet, F_D is the damping force acting on the body, and f is an external force disturbance see (Fig. 3.2.1). The linearized equation of motion for the suspended body is

$$m\ \delta\ddot{x}(t) = K_x \delta x(t) - K_i \delta i(t) - C\delta\dot{x}(t) + f \tag{3.1.2}$$

where

$$K_x = \frac{\partial}{\partial x}(F_A) \tag{3.1.3}$$

and

$$K_i = \frac{\partial}{\partial i}(F_A) \tag{3.1.4}$$

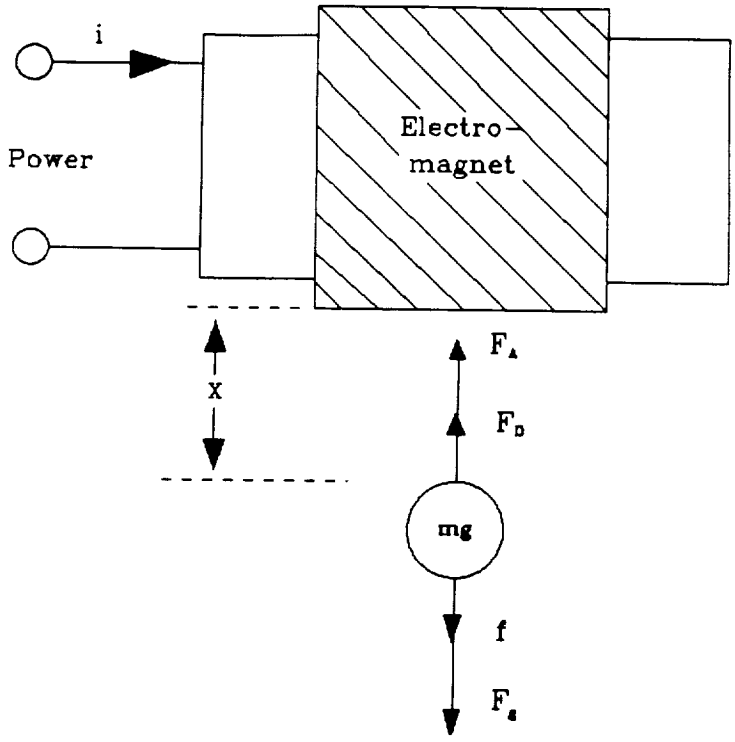

Figure 3.1.1 Schematic of Single Degree-of-Freedom Magnetic Suspension and Balance System.

The linearized governing equation of the electromagnetic coil is the sum of the voltage drop across the coil resistance and the voltage across the inductance (Ref. 6).

$$\delta V(t) = \delta i(t)R + L\frac{d}{dt}[\delta i(t)] + K_c \delta x(t) \tag{3.1.5}$$

where

$$K_c = i_0 \frac{d}{dx}(L) \tag{3.1.6}$$

Transforming equations 3.1.2 and 3.1.5 to the Laplacian S-domain, they become

$$mS^2\Delta X = K_x\Delta X - K_i\Delta I - CS\Delta X + f \tag{3.1.7}$$

$$\Delta V = R\Delta I + LS\Delta I + K_c S\Delta X \tag{3.1.8}$$

Combining equation 3.1.7 and 3.1.8, the Plant Transfer Function (Ref. 6) becomes

$$\Delta X = \frac{-\frac{K_i}{mL}\Delta V + \frac{R}{mL}\left[1 + \frac{L}{R}S\right] f}{S^3 + S^2\left[\frac{R}{L} + \frac{C}{m}\right] + S\left[\frac{CR}{mL} - \frac{K_x}{m} - \frac{K_i K_c}{mL}\right] - \frac{RK_x}{Lm}} \tag{3.1.9}$$

Due to the distance of the model from the electromagnets, K_c is very small, therefore it is equal to zero, and since the aerodynamic forces are negligible, C is very small and it is equal to zero, therefore, equation 3.1.9 simplifies to

$$\Delta X = \frac{-\frac{K_i}{mL}\Delta V + \frac{R}{mL}\left[1 + \frac{L}{R}S\right] f}{\left[S^2 - \frac{K_x}{m}\right]\left[S + \frac{R}{L}\right]} \tag{3.1.10}$$

3.2 Five Degree-of-Freedom System

3.2.1 Equations of Motion

Five electromagnets is the minimum number of actuators required since five degrees-of-freedom are being controlled. A representation of this system is shown in figure 3.2.1. The motion of the core (cylinder) is defined by the body fixed axes $\bar{x}$, $\bar{y}$, $\bar{z}$ that define the motion of the core with respect to fixed inertial axes x, y, z. The electromagnet array is also defined by fixed inertial axes x_b, y_b, z_b. The x, y axes are parallel to the x_b, y_b axes; z and z_b are coincident.

The origins of the two axes are separated by the distance h (Fig. 3.2.1). Deriving the following equations (Ref. 8), the following assumptions where used: (1) The core is a rigid body, (2) the core has negligible products of inertia, and (3) there is no motion about the $\bar{x}$ axis. $\bar{x}$ is an axis of symmetry so that:

$$I_{\bar{y}} = I_{\bar{z}} = I_c \tag{3.2.1.1}$$

In core coordinates, the momentum of the core is

$$[\bar{H}] = (I)\,[\bar{\Omega}] \tag{3.2.1.2}$$

where

$$(I) = \begin{bmatrix} I_{\bar{x}} & 0 & 0 \\ 0 & I_c & 0 \\ 0 & 0 & I_c \end{bmatrix} \tag{3.2.1.3}$$

and

$$[\Omega] = [0 \;\; \Omega_{\bar{y}} \;\; \Omega_{\bar{z}}] \tag{3.2.1.4}$$

The total torque, $[T]$, about the core center of mass is

$$[\bar{T}] = \frac{d[\bar{H}]}{dt} = (I)\,\frac{d[\bar{\Omega}]}{dt} + [\bar{\Omega}] \times \{\,(I)\,[\bar{\Omega}]\,\} \tag{3.2.1.5}$$

the total torque can be written as

$$[\bar{T}\,] = [\bar{T}_m] + [\bar{T}_d] \tag{3.2.1.6}$$

where $[\bar{T}_m]$ are the control torques produced by the electromagnets, $[\bar{T}_d]$ are the external disturbance torques. From equation 3.2.1.2 and with the assumption that $\Omega_{\bar{x}} = 0$, the cross

product term becomes zero and

$$\frac{d\bar{\Omega}}{dt} = \left[\frac{1}{I_c}\right][\bar{T}] \tag{3.2.1.7}$$

The core angular rates are obtained by integrating equation 3.2.1.7.

The forces on the core, in core coordinates are

$$[\bar{F}] = m_c \left\{ \frac{d[\bar{V}]}{dt} + [\bar{\Omega}]\,[\bar{V}] \right\} \tag{3.2.1.8}$$

where m_c is the core mass, $[\bar{V}]$ is the core velocity. $[\bar{F}]$ can be written as

$$[\bar{F}] = [\bar{F}_m] + [\bar{F}_d] \tag{3.2.1.9}$$

where $[\bar{F}_m]$ are the control forces produced by the electromagnets, $[\bar{F}_d]$ are the disturbance forces. The core translational rates become

$$[V] = [T_m]^{-1}\,[\bar{V}] \tag{3.2.1.10}$$

$[T_m]^{-1}$ gives a transformation matrix from core coordinates to inertial space. Integrating equation 3.2.1.8, the displacement of core center of mass is obtained. The assumption is made that the rates will be small and their products can be neglected since the core is actively controlled, therefore, the result is

$$\frac{d[\bar{V}]}{dt} = \left[\frac{1}{m_c}\right]\,[\bar{F}] \tag{3.2.1.11}$$

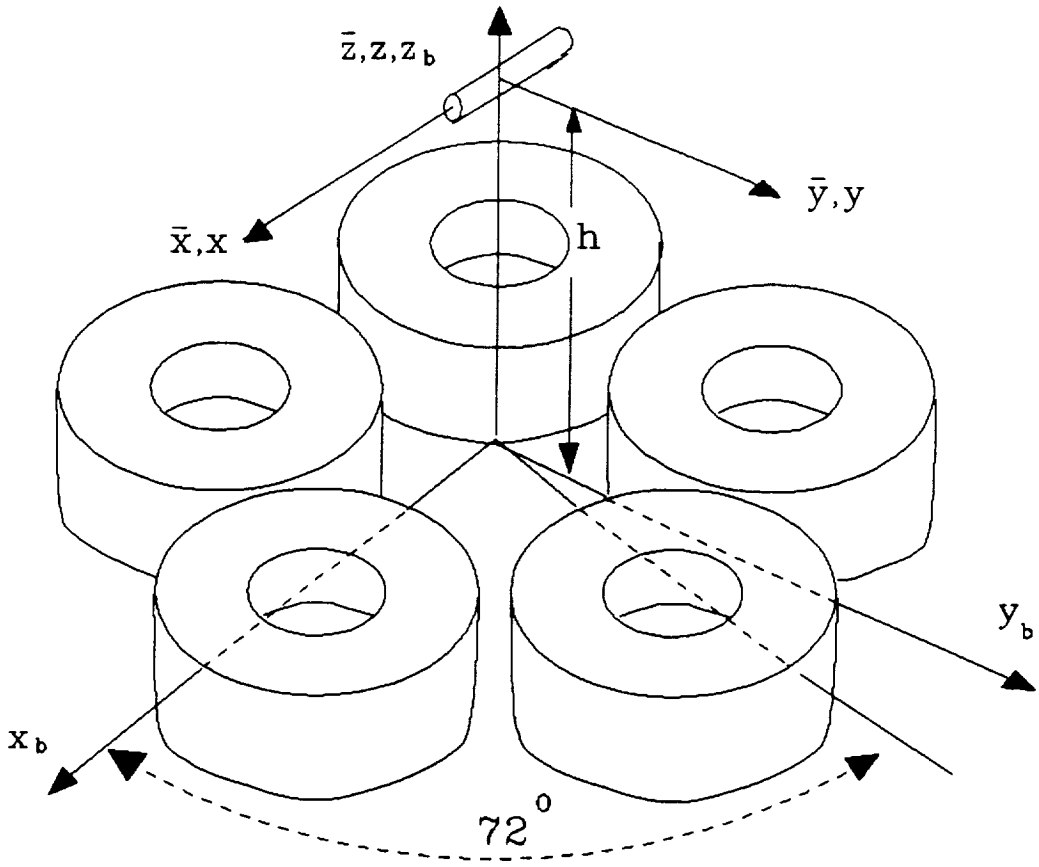

Figure 3.2.1 Initial coordinate system alignment for Large-Gap Magnetic Suspension System.

3.2.2 Magnetic Forces and Torques

In x, y, z coordinate system, the torque on a magnetic core in a nonuniform magnetic field (see Ref. 8) can be written as

$$[T] = \int_{Vol} \{[M] \times [B]\}\, d(Vol) \qquad (3.2.2.1)$$

where the integral is taken over the core volume, M is the core magnetization in Amp/meter, B is the flux density in Tesla, Vol is the volume in cubic meters and the torque T is in Newton-

meters. The force on the core is written as

$$[F] = \int_{vol} \{[M] . \nabla\} [B] \, d(Vol) \tag{3.2.2.2}$$

where F is in Newtons and ∇ is the gradient operator that is defined as

$$\nabla = \frac{\partial}{\partial x} \hat{i} + \frac{\partial}{\partial y} \hat{j} + \frac{\partial}{\partial z} \hat{k} \tag{3.2.2.3}$$

The size of the core is small relative to the electromagnets and the air-gaps, therefore, assuming that the field gradient components are uniform over the volume of the core, an approximation of the forces and torques can be obtained, so the torque becomes

$$[T] = Vol \, [M] \times [B] \tag{3.2.2.4}$$

where $[M]$ is the magnetization. After some simplification and notation change, the force becomes

$$[F] = Vol \, [\partial B] \, [\bar{M}] \tag{3.2.2.5}$$

where

$$[\partial B] = \begin{bmatrix} B_{xx} & B_{xy} & B_{xz} \\ B_{yx} & B_{yy} & B_{yz} \\ B_{zx} & B_{zy} & B_{zz} \end{bmatrix} \tag{3.2.2.6}$$

Maxwell equations apply in the core region, therefore $\nabla \times B = 0$ which results in: $B_{xy} = B_{yx}$, $B_{xz} = B_{zx}$, $B_{yz} = B_{zy}$ Also $\nabla . B = 0$ results in: $B_{xx} + B_{yy} + B_{zz} = 0$

In equations 3.2.2.5 and 3.2.2.6, $[\bar{M}]$ is defined in core coordinates while $[B]$ is in inertial coordinates. In order to calculate the torque in core coordinates, $[B]$ has to be

transformed into the same coordinate system, this results in

$$[T] = Vol\ [\bar{M}]\ [T_m] \times [B] \tag{3.2.2.7}$$

and the force transformed back into core coordinates

$$[\bar{F}] = Vol\ [T_m]\ [\partial B]\ [T_m]^{-1}\ [\bar{M}] \tag{3.2.2.8}$$

3.2.3 System Equations

The magnetic forces and torques are combined with the permanent magnet core equations of motion to produce a model of the magnetic suspension system. The following are the resulting system equations

$$\frac{d[\bar{V}]}{dt} = \left[\frac{1}{m_c}\right] \left\{Vol\left([T_m]\ [\partial B]\ [T_m]^{-1}\ [\bar{M}]\right) + \bar{F}_d\right\} \tag{3.2.3.1}$$

$$\frac{d[\bar{\Omega}]}{dt} = \left[\frac{1}{\bar{I}_c}\right] \left\{Vol\left([\bar{M}][T_m] \times [B]\right) + [\bar{T}_d]\right\} \tag{3.2.3.2}$$

Equation 3.2.3.1 and 3.2.3.2 are the equations of motion in core coordinates in terms of $[B]$ and $[\partial B]$. In inertial coordinates $[B]$ can be written as

$$[B] = \left[\frac{1}{I_{max}}\right] [K_B]\ [I] \tag{3.2.3.3}$$

where $[K_B]$ is a 3 x 5 matrix whose elements represent the values of $[B]$ produced by a corresponding coil driven by the maximum current, I_{max}. By arranging the elements of $[\partial B]$ as a column vector, the gradients can be put in the same form which results in

$$[\partial B] = \left[\frac{1}{I_{max}}\right] [K_{\partial B}] [I] \tag{3.2.3.4}$$

where $[\partial B]$ is a nine element column vector containing the gradients of $[B]$, $[K_{\partial B}]$ is 9x5 matrix whose elements represent the values of $[\partial B]$ produced by a corresponding coil driven by the maximum current, each element can be written as

$$[B_{xx}] = \left[\frac{1}{I_{max}}\right] [K_{xx}] [I] \tag{3.2.3.5}$$

where $[K_{xx}]$ is a 1 x 5 matrix containing values of B_{xx} produced by a corresponding coil.

This model is nonlinear because of the combination of states resulting from the coordinate transformations and has the following form

$$\dot{X} = f(x,u) \tag{3.2.3.6}$$

where x is given by

$$X^T = \left[\bar{\Omega}_y \;\; \bar{\Omega}_z \;\; \theta_y \;\; \theta_z \;\; \bar{V}_x \;\; \bar{V}_y \;\; \bar{V}_z \;\; x \;\; y \;\; z \right] \tag{3.2.3.7}$$

and the input u is given by

$$u^T = \left[I_1 \;\; I_2 \;\; I_3 \;\; I_4 \;\; I_5 \right] \tag{3.2.3.8}$$

The equations of motion can be linearized around the nominal operating point X_0, I_0 by performing a Taylor Series Expansion. Ignoring second order terms and subtracting out X_0

results in

$$\delta\dot{X} = \bar{A}\delta X + \bar{B}\delta I \tag{3.2.3.9}$$

where

$$\bar{A} = \left[\frac{\partial(\dot{X})}{\partial X}\right]_{X_0, I_0} \tag{3.2.3.10}$$

and

$$\bar{B} = \left[\frac{\partial(\dot{X})}{\partial I}\right]_{X_0, I_0} \tag{3.2.3.11}$$

where $\dot{X}$ has the following form

$$\dot{X} = F\left\{\left[\frac{\bar{T}}{\bar{F}}\right]\right\} \tag{3.2.3.12}$$

The A matrix of Eq. 3.2.3.10 has the following form

$$\bar{A} = \begin{bmatrix} \bar{T}_{y\bar{0}_y} & \bar{T}_{y\bar{0}_x} & \bar{T}_{y\theta_y} & \bar{T}_{y\theta_x} & \bar{T}_{y\bar{V}_y} & \bar{T}_{y\bar{V}_y} & \bar{T}_{y\bar{V}_x} & \bar{T}_{yx} & \bar{T}_{yy} & \bar{T}_{yz} \\ \bar{T}_{z\bar{0}_y} & \bar{T}_{z\bar{0}_x} & . & . & . & & & & & \\ \bar{\Omega}_{y\bar{0}_y} & \bar{\Omega}_{y\bar{0}_x} & \bar{\Omega}_{y\theta_y} & . & . & & & & & \\ \bar{\Omega}_{z\bar{0}_y} & . & . & . & . & & & & & \\ \bar{F}_{x\bar{0}_y} & . & . & . & . & & & & & \\ \bar{F}_{y\bar{0}_y} & . & . & . & . & & & & & \\ \bar{F}_{z\bar{0}_y} & . & . & . & . & & & & & \\ \bar{V}_{x\bar{0}_y} & . & . & . & . & & & & & \\ \bar{V}_{y\bar{0}_y} & . & . & . & . & & & & & \\ \bar{V}_{z\bar{0}_y} & . & . & . & . & & & & & \end{bmatrix} \tag{3.2.3.13}$$

which reduces to the following

$$\bar{A} = \begin{bmatrix} 0 & 0 & T_{y\theta_y} & T_{y\theta_z} & 0 & 0 & 0 & T_{yx} & T_{yy} & T_{yz} \\ 0 & 0 & T_{z\theta_y} & T_{z\theta_z} & 0 & 0 & 0 & T_{zx} & T_{zy} & T_{zz} \\ 1 & 0 & 0 & 0 & 0 & 0 & 0 & 0 & 0 & 0 \\ 0 & 1 & 0 & 0 & 0 & 0 & 0 & 0 & 0 & 0 \\ 0 & 0 & F_{x\theta_y} & F_{x\theta_z} & 0 & 0 & 0 & F_{xx} & F_{xy} & F_{xz} \\ 0 & 0 & F_{y\theta_y} & F_{y\theta_z} & 0 & 0 & 0 & F_{yx} & F_{yy} & F_{yz} \\ 0 & 0 & F_{z\theta_y} & F_{z\theta_z} & 0 & 0 & 0 & F_{zx} & F_{zy} & F_{zz} \\ 0 & 0 & 0 & 0 & 1 & 0 & 0 & 0 & 0 & 0 \\ 0 & 0 & 0 & 0 & 0 & 1 & 0 & 0 & 0 & 0 \\ 0 & 0 & 0 & 0 & 0 & 0 & 1 & 0 & 0 & 0 \end{bmatrix} \qquad (3.2.3.14)$$

where the following notation has been used for simplification

$$\frac{\partial F_i}{\partial j} = F_{ij} \qquad (3.2.3.15)$$

At initial alignment and equilibrium, $\bar{F}_x = \bar{F}_y = \bar{T}_y = \bar{T}_z = 0$.

Equation 3.2.3.11 takes the following form

$$\bar{B} = \begin{bmatrix} \bar{T}_{yI_1} & \bar{T}_{yI_2} & \bar{T}_{yI_3} & \bar{T}_{yI_4} & \bar{T}_{yI_5} \\ \bar{T}_{zI_1} & \bar{T}_{zI_2} & . & . & . \\ \bar{\Omega}_{yI_1} & . & . & & \\ . & . & & & \\ . & & & & \\ . & & & & \end{bmatrix} \qquad (3.2.3.16)$$

Terms involving $\bar{\Omega}$ and $\bar{V}$ are neglected.

Taking the first term of the $\bar{B}$ matrix

$$\frac{\partial \bar{T}_y}{\partial I_1} = (vol)\, M_{\bar{x}} \left[-\theta_y \frac{\partial B_x}{I_1} - B_x \frac{\partial \theta_y}{I_1} - \frac{\partial B_z}{\partial I_1} \right] \qquad (3.2.3.17)$$

The term $\frac{\partial \theta_2}{\partial I_1} = 0$ also, when evaluating Eq. 3.2.3.11 at X_0, the terms with θ_y and θ_z drop out.

The coefficients of the above A and B matrices are given in more detail in Appendix A along with their numerical values.

CHAPTER 4

SINGLE DEGREE OF FREEDOM SIMULATION

4.1 System Selection and Transfer functions

To assist in determination of the gains of the five degree-of-freedom system an approximate value needed to be found prior to full simulation. Therefore, a transfer function was found for a single-input single-output (SISO) system using values from the yaw component of the complete system. The eigen-values and eigen-vectors that represent the mode shapes and frequencies are presented in Table 4.1.1. A DPA controller was added to compensate this unstable system. An approximate gain that can be used to estimate the gains of the remaining degrees-of-freedom can then be determined. This uncontrolled SISO system has eight poles and eight zeros that cancel each other out due to the other uncoupled degrees-of-freedom, leaving two poles that compose the system's transfer function denominator. Using MATLAB, a transfer function of the yaw degree-of-freedom was obtained from the overall system, setting the derivatives equal to zero, a constant value equal to .3019 was obtained which is equal to k/c where k is the gain, therefore .3019 was multiplied by c to obtain k equal to 49.9453. With these results, the transfer function is second order and takes the following form

$$G(S) = \frac{49.9453}{aS^2 + bS + c} \qquad (4.1.1)$$

where a = 1, b = 0, and c = -165.4233. These values of the yaw degree-of-freedom were obtained from the system matrix of the overall system shown in Appendix A. The following bode plots were achieved from the overall state-space matrices for the yaw degree-of-freedom and the above transfer function which prove that they are identical.

Mode	1		2		3	
Eigenvalue	13.6918	-13.6918	1.7843i	-1.7843i	12.86177	-12.8617
Ω_y	-0.9957	0.9957	-0.7968	-0.7968	0	0
Ω_z	0	0	0	0	0.9970	0.9970
θ_y	-0.0727	0.0727	0.4466i	-0.4466i	0	0
θ_z	0	0	0	0	0.0775	-0.0775
V_x	0.058	0.058	-0.3551	-0.3551	0	0
V_y	0	0	0	0	0	0
V_z	0	0	0	0	0	0
x	0.0042	-0.0042	0.1990i	-0.1990i	0	0
y	0	0	0	0	0	0
z	0	0	0	0	0	0

Mode	4		5	
Eigenvalue	5.0313i	-5.0313i	2.5058	-2.5058
Ω_y	0	0	0	0
Ω_z	0	0	0	0
θ_y	0	0	0	0
θ_z	0	0	0	0
V_x	0	0	0	0
V_y	0	0	0.9288	0.9288
V_z	0.9808	0.9808	0	0
x	0	0	0	0
y	0	0	0.3707	0.3707
z	-0.1949i	-0.1949i	0	0

Table 4.1 Eigen-values and Eigen-vectors of the overall Magnetic Suspension System.

Observing table 4.1, the modes are identified as follows: The translational divergence in the y direction is Mode 5. The undamped vertical motion (mass + spring stiffness type) is Mode 4. Mode 3 is the "compass needle" term, in this case relating to divergent rotation about the z axis. Mode 1 arises due to the compass needle term about the y axis, but couples into translation in the x-direction. Mode 2 is due to the translational divergence in the x-direction, but couples into pitching moment strong enough to produce an oscillatory mode.

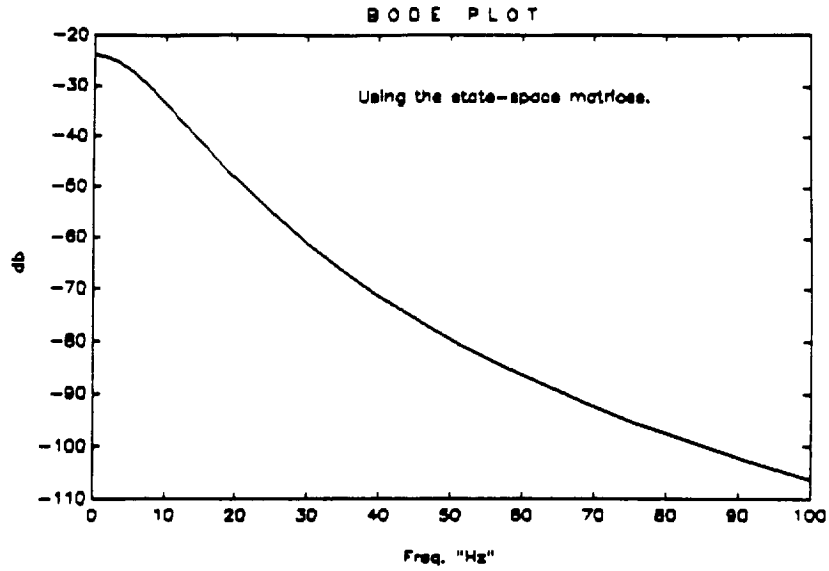

Figure 4.1.1 Bode plot of the yaw degree-of-freedom from the overall state-space matrices.

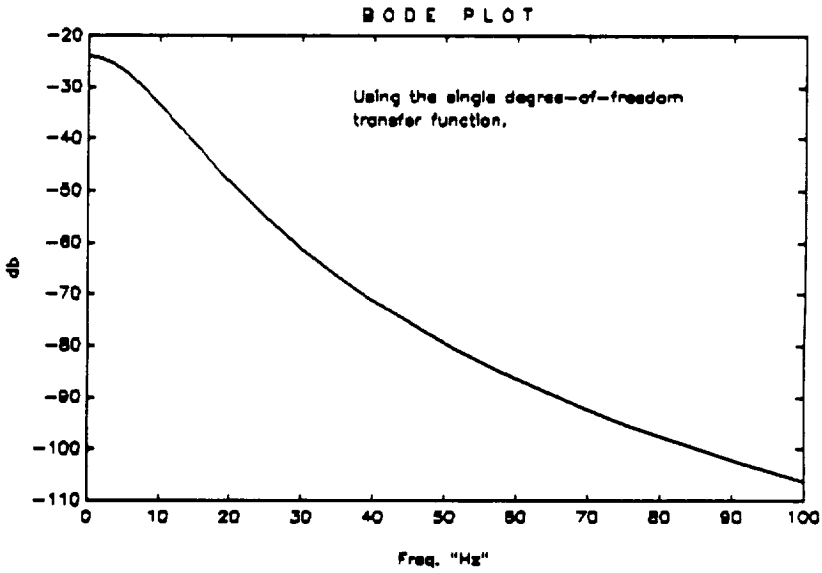

Figure 4.1.2 Bode plot of equation 4.1.1.

The two types of controllers that were used in order to determine which one is better suited for this system are the DPA and the PID controllers. The DPA transfer function has the following form

$$G(S) = \frac{(1 + nTS)^2}{(1 + TS)^2} \tag{4.1.2}$$

Equations 4.1.1 and 4.1.2 are combined to form the following SISO open-loop compensated transfer function without the power supply.

$$G(S) = \frac{(1 + nTS)^2}{(1 + TS)^2 (aS^2 + bS + c)} \tag{4.1.3}$$

The transfer function of the PID takes the following form

$$G(S) = \frac{aS^2 + bS + c}{S} \tag{4.1.4}$$

to obtain PD control, c is set equal to zero. The value of a and b were taken to equal 1 and 18 respectively. If the value of b is increased, the system becomes stiffer. Multiplying (Eq. 4.1.1) with (Eq. 4.1.4) also produces a compensated open-loop system but with the PD controller instead.

The values from the coupling matrix (Ref. 4) of the field gradients for the five-degree-of-freedom LGMSS were used to calculate the current distribution. It is found that the required B_{xx} to suspend equal 0.0962 T/m, therefore solving the following equation (Eq. 3.2.3.5)

$$\begin{bmatrix} K_{y_1} & \cdots & K_{y_5} \\ K_{z1} & \cdots & \\ K_{(xx)_1} & \cdots & \\ K_{(xy)_1} & \cdots & \\ K_{(xz)_1} & \cdots & \end{bmatrix} \begin{bmatrix} I_1 \\ \cdot \\ \cdot \\ \cdot \\ \cdot \\ I_5 \end{bmatrix} = \begin{bmatrix} B_y \\ B_z \\ B_{xx} \\ B_{xy} \\ B_{xz} \end{bmatrix} \tag{4.1.5}$$

substituting for B_y; B_z; B_{xx}; $B_{xy} = 0$ and $B_{xz} = 0.0962$, gives the current distribution required as

$$I = \begin{bmatrix} -0.7753 \\ -0.2417 \\ 0.6293 \\ 0.6293 \\ -0.2417 \end{bmatrix} \tag{4.1.6}$$

Using the equations of the forces and torques (Appendix A), the values of B_y and B_{xz} were found with the following procedure. In equilibrium, the only force on the core is along the z axis and is equal to the core weight

$$F_{\bar{z}} = m_c\, g \tag{4.1.7}$$

where g is the acceleration of gravity. and from the equations in Appendix A

$$B_{xz} = \frac{m_c\, g}{(Vol)\, M_{\bar{z}}} \tag{4.1.8}$$

The power supply transfer function is

$$G(S) = \frac{1}{S + 130} \tag{4.1.9}$$

where the power supply pole located at -130.

In the Single Degree-of-Freedom transfer function Eq. 4.1.1, the large negative number in the denominator indicates considerable spring stiffness and shows the presence of instability.

A B_{yd} value of 1.0001 is multiplied by Eq. 4.1.1 and Eq. 4.1.9 to produce the following uncompensated system transfer function

$$G(S) = \frac{.6293}{.0077S^3 + S^2 - 1.2738S - 165.42} \tag{4.1.10}$$

The value of B_{yd} was obtained by multiplying each value of the second column of the decoupling matrix by Eq.4.1.9, the five resulting values were multiplied by the values of B_y for each coil (Table A.1), and the sum of the results produced the value of B_{yd}.

The DPA transfer function is

$$G(S) = \frac{.0014S^2 + .0741S + 1}{.0002S^2 + .0074S + 1} \tag{4.1.11}$$

Eq. 4.1.10 and Eq. 4.1.11 are multiplied to produce the following open-loop compensated transfer function with DPA controller

$$G(S) = \frac{0.637\ S^2 + 3.5675S + 49.9453}{9.81 \times 10^{-8}S^5 + 6.77 \times 10^{-5}S^4 + .015S^3 + .989S^2 - 2.4541S - 165.42} \tag{4.1.12}$$

The following is the PD controller equation

$$G(S) = S + 18 \tag{4.1.13}$$

multiplying equation 4.1.10 and 4.1.13, the open-loop compensated transfer function with the PD controller is

$$G(S) = \frac{12.4863S + 224.754}{.0077S^3 + S^2 - 1.2725S - 165.42} \qquad (4.1.14)$$

Equations 4.1.12 and 4.1.14 are the sources for calculating the root-locus of the closed-loop system in order to determine the approximate gain that produces stability.

The determination of the stability of the system was accomplished by the use of the root-locus method. The compensated open-loop transfer function had to be derived by Eq. 4.1.1 and Eq. 4.1.2. In Eq. 4.1.2, the value of n was taken to be equal 10, and the optimal value of T that produced a root-locus which gives a stable system with sufficient amount of gain is equal to 0.0036. This value of T helped producing a root-locus of a system that becomes stable with sufficient amount of gain. The location of the single power supply pole was determined by multiplying the maximum open-loop plant eigenvalue of 13 by 10. After the location of the poles and zeros of the controller and the power supply were established, the appropriate root-locus was plotted in (Fig. 4.1.3 and Fig. 4.1.4). To achieve the stability of the system with the desired damping value, a gain of about 7 was chosen.

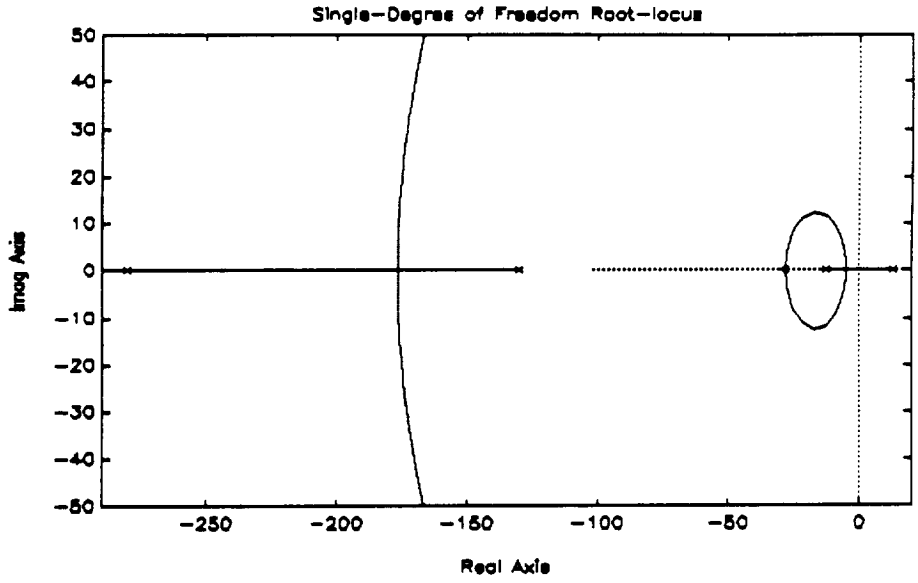

Figure 4.1.3 Root-Locus plot of the overall single degree of freedom system. The value of the gain K = 7.

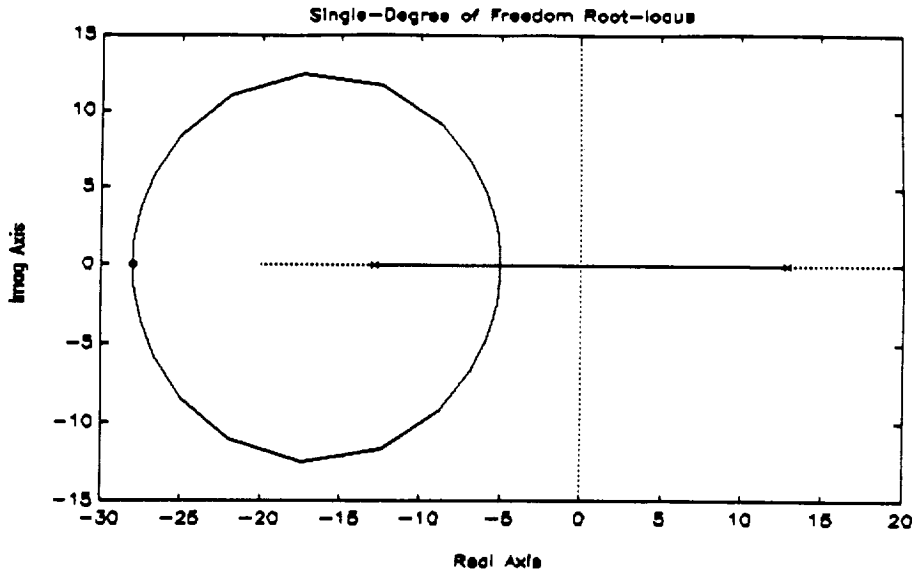

Figure 4.1.4 Root-locus plot of the overall system with zeros and poles closest to the origin. The value of the gain K = 7.

4.2 The Step Response

To obtain the step response of the yaw mode, the closed-loop transfer function has to be evaluated. This closed loop transfer function has the following form

$$G(S) = \frac{KH(S)}{1 + KH(S)} \tag{4.2.1}$$

where K is the gain.

Using Eq. 4.2.1, the closed-loop transfer functions of the DPA and PD controller respectively were obtained and took the following form

$$G(S) = \frac{6.37 \times 10^{-4} S^2 + .3568S + 49.9453}{9.8 \times 10^{-8} S^5 + .0001S^4 + .0148S^3 + 1.435S^2 + 22.529S + 184.194} \tag{4.2.2}$$

$$G(S) = \frac{49.9453}{.00769S^3 + S^2 + 36.187S + 508.838} \qquad (4.2.3)$$

where the denominator of the above two transfer functions has the gain already included.

The step response curve corresponding to Eq. 4.2.2 using the DPA Controller is Fig. 4.3.1. Restricting the overshoot to five percent, the amount of gain (K) required to reach this objective was 7, and the settling time was obtained to equal .24 seconds which is quite rapid. This value of gain is the target quantity that satisfies the damping criteria of .6963 obtained from the root-locus plot (Fig. 4.1.1), which is close to the optimum value of .707. Increasing the above value of gain, the overshoot becomes smaller than the five percent criteria above but the damping value acquires very small change, eventually, the system becomes overdamped.

Looking at Fig. 4.2.2 which corresponds to the system with PD control, It is observed that the overshoot falls within the five percent criteria and has a rapid settling time also. This PD controller appear to be a good reliable alternative for this system since it exhibits a satisfactory behavior.

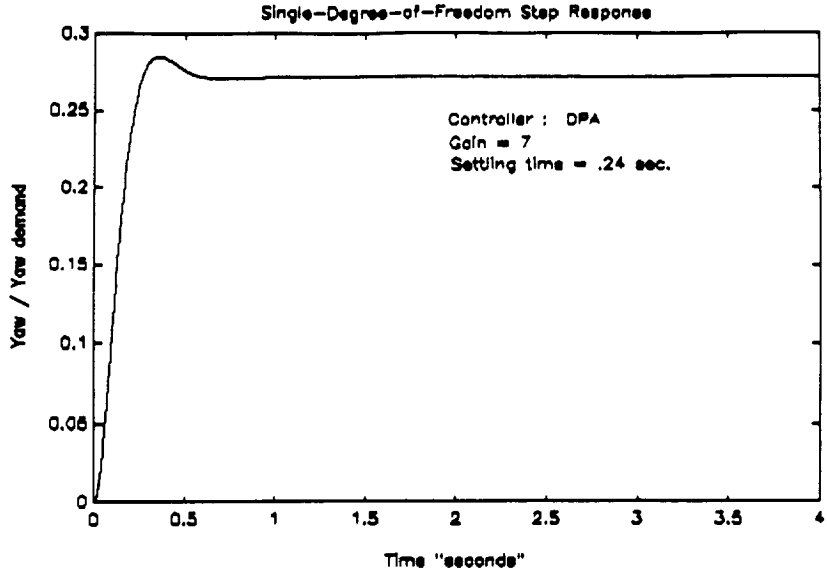

Figure 4.2.1 Step response curve of single degree-of-freedom system with Dual Phase Advance controller.

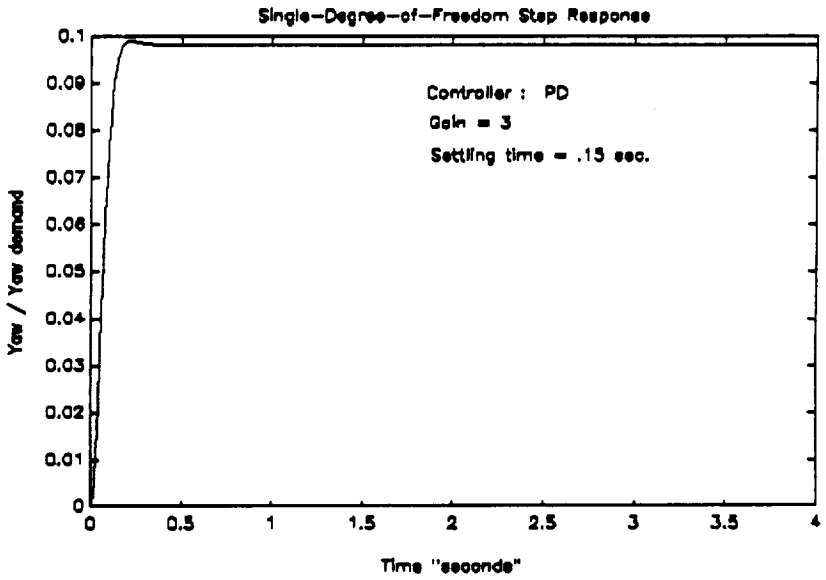

Figure 4.2.2 Step response curve of single degree-of-freedom system with PD controller.

CHAPTER 5

COMPARISON OF CONTROLLERS

5.1 White Noise

The single degree-of-freedom Magnetic Suspension and Balance System simulation was used to examine the effect of random noise on the Phase Advanced and PID controllers. The existing simulation program that was used to compare different kinds of controllers (Ref. 5) was modified to accommodate the noise equations and extra graphic capability. Random numbers between zero and one were inserted in the normal or Gaussian function (Ref. 11) to generate uniformly distributed white noise, which was taken and added to each of the controller's inputs where the sensor is located, Figure 5.1.1 shows where the noise was introduced. The output data generated above for each of the controllers was used to calculate their root mean square (RMS) value.

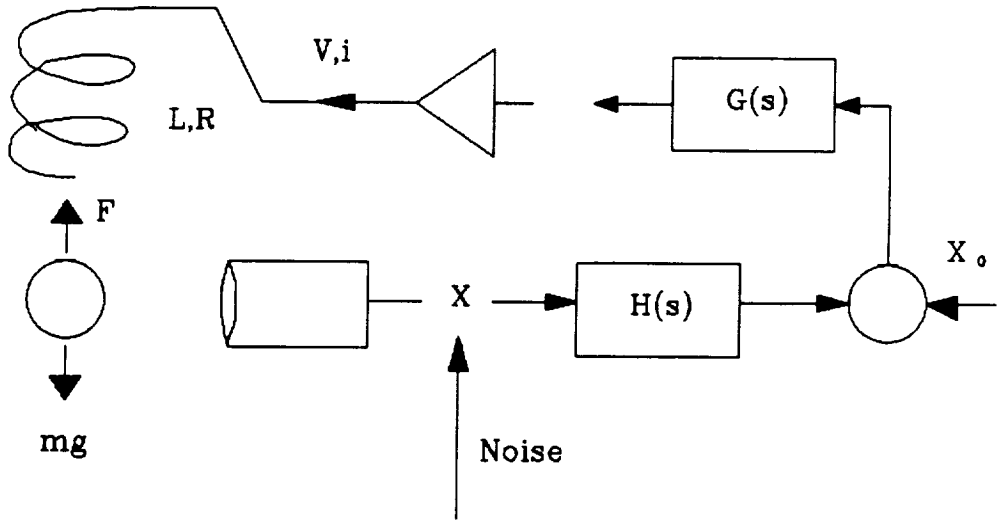

Figure 5.1.1 Magnetic suspension controller arrangement with noise.

The Gaussian function is

$$\frac{1}{\sqrt{2\pi\sigma^2}}\, e^{\left(\frac{-(x-\bar{x})^2}{2\sigma^2}\right)} \qquad (5.1.1)$$

where σ is the variance and $\bar{x}$ is the median.

To demonstrate the noise distribution graphically, a Fourier Transform algorithm to estimate the power spectra of signals was used with the assistance of Matlab (Ref. 13). Eq. 5.1.1 was incorporated in the single degree of freedom program (Appendix C) where the white noise data was produced. This data was then used in the Fourier transform algorithm to plot the power spectral density (Fig 5.1.2) which shows reasonably good white noise, even though only one thousand points were used.

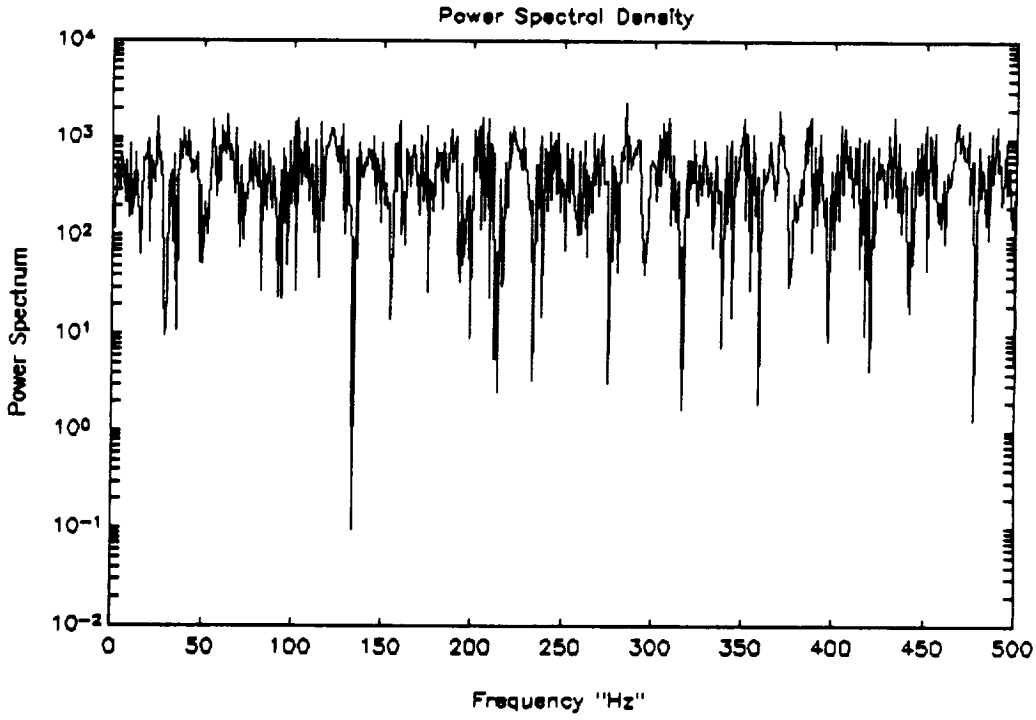

Figure 5.1.2 White noise power spectral density plot.

The root mean square was calculated using the following equation (Ref. 12)

$$I_{RMS} = \sqrt{\frac{\int_0^T I^2(t)\,dt}{T}} \tag{5.1.2}$$

where T is the time. Equation 5.1.2 produces the same results as the following standard deviation equation

$$\Gamma = \sqrt{\frac{\Sigma (x-\bar{x})^2}{n}} \tag{5.1.3}$$

where Γ is the standard deviation, $\bar{x}$ is the mean and n is the number of points.

To evaluate the I_{RMS} of the DPA and the PID controllers, the program of the Single-Degree-of-Freedom system (Appendix C) was used. The standard deviation equation (Eq. 5.1.3) was incorporated in this program to perform this operation.

5.2 Dual Phase Advance (DPA) Controller

To test the effect of the random white noise on this controller, random numbers were generated in the program (Appendix C), processed by equation (Eq. 5.1.1) and were incorporated in the DPA subroutine, the resulting output was used to produce the power spectral density plot (Fig. 5.2.1) which shows the presence of noise. The single-degree-of-freedom magnetic suspension system simulation program (Ref. 5) tested the behavior of various types of controllers on the suspension of spherical metal object. In this simulation, the aim was to obtain the value of gain that produced five percent position over-shoot. For the DPA controller, the value was

found to equal 2784. This value of gain is then used in the modified program (Appendix C) to evaluate the RMS of this particular controller, and the resulting value is .145. In the simulation program (Appendix C), the output data including the noise had a large numbers, therefore it was multiplied by .0001 for scaling. Looking at Fig. 5.2.2, it is observed that the resonant frequency of the order of 10 Hz.

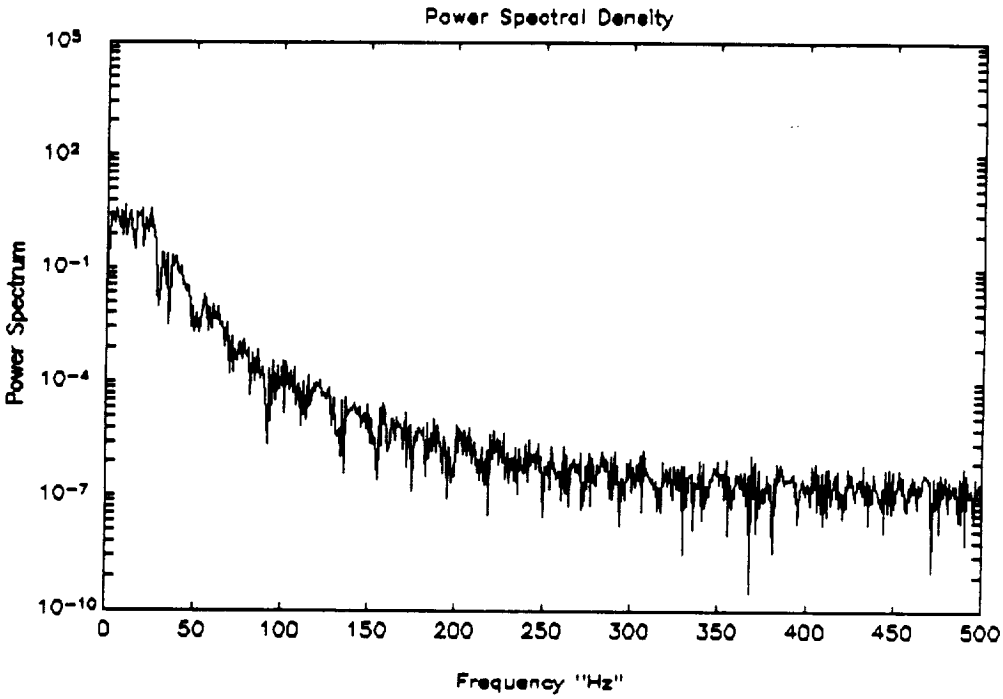

Figure 5.2.1 Power spectral density of the single degree-of-freedom system with Dual Phase Advance controller.

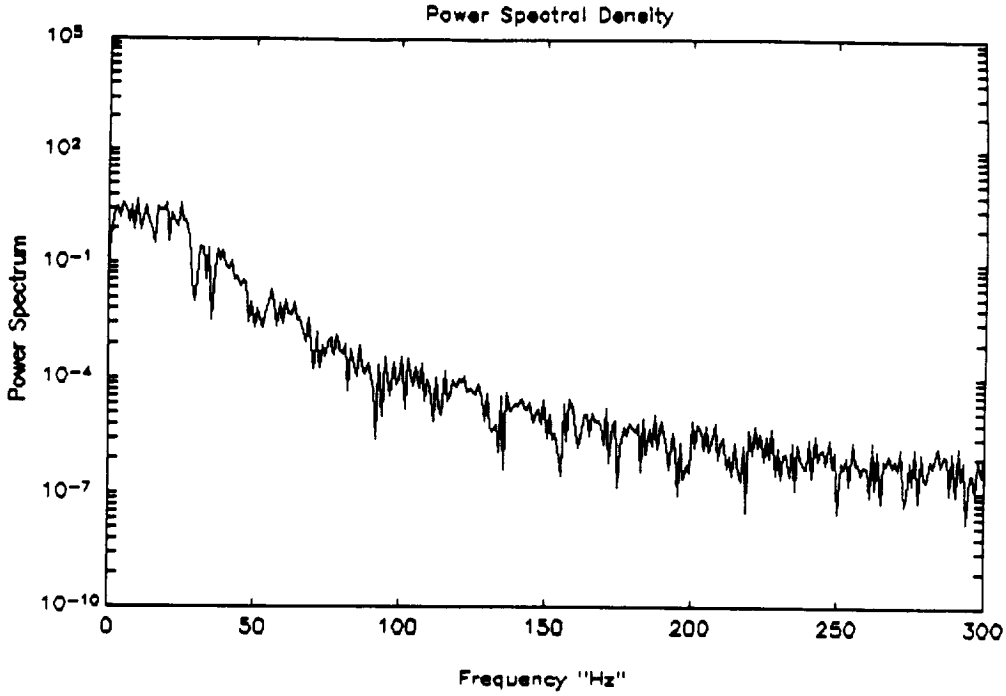

Figure 5.2.2 Power spectral density of single degree-of-freedom system with Dual Phase Advance controller, and smaller frequency range.

5.3 PD Controller

Applying the same principles as the DPA controller, the gain value used for the PD controller to accomplish the five percent overshoot is 396. Using this value, the resulting RMS is .6136 for this controller where the data that included the noise was also multiplied by .0001 for scaling. This RMS value is about four times bigger than the DPA controller RMS value. (Fig. 5.3.1) shows the power spectral density plot with noise present. This plot shows that the resonant frequency is also of the order of 10 Hz.

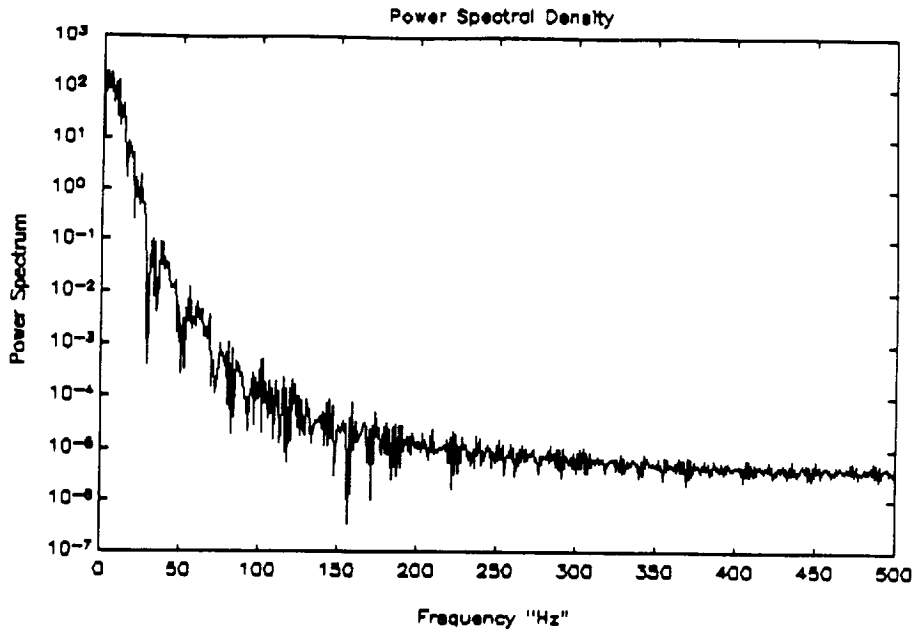

Figure 5.3.1 Power spectral density plot of single degree-of-freedom system with PD controller.

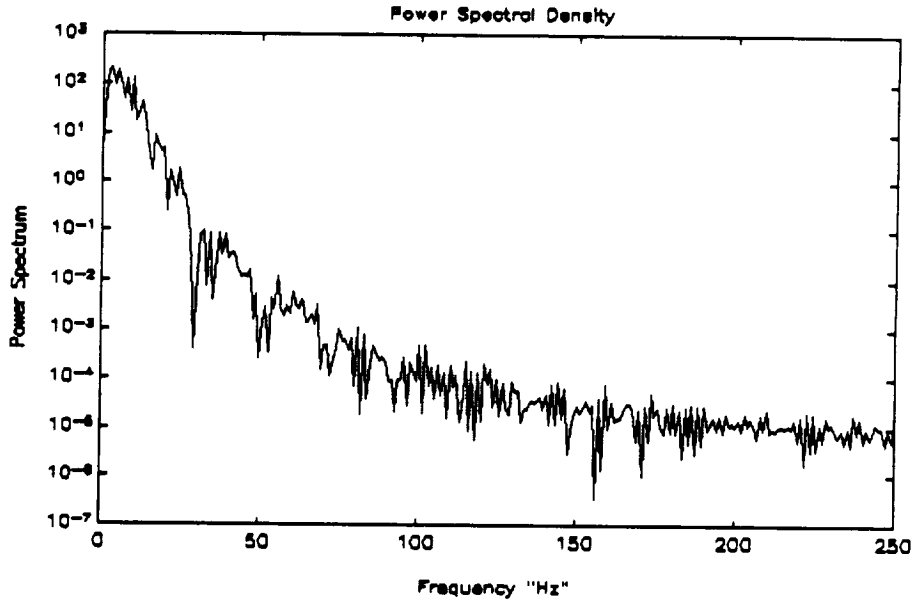

Figure 5.3.2 Power spectral density of single degree-of-freedom system with PD controller and smaller frequency range.

5.4 Comparison:

Executing the single-degree-of-freedom simulation program (Appendix C) with the noise generation, the output of the PD and the DPA controllers was Fourier Transformed to generate power spectral density plots. Examining the plots, it is observed from Fig. 5.2.1 and Fig. 5.3.1 that the resonant frequency of both the DPA and the PD controllers are of the same order of about 10 Hz. Within the simulation program, the RMS value both controllers was evaluated where the PD controller produced a value about four times larger than the DPA controllers. Considering the over-shoot and settling-time behavior of both controllers in chapter 4, the DPA controller produced a quick settling-time while maintaining the five percent over-shoot criteria. Mean while, the PD controller also had very quick settling-time while maintaining the five percent over-shoot criteria.

Therefore due to the results mentioned above, the two controllers have proved to be prime candidates for the magnetic suspension system. But the DPA controller has the edge with its noise performance (RMS value) and permits much higher gain before it becomes unstable. Based on this criteria, the DPA controller was the choice for this system.

CHAPTER 6

FIVE DEGREE-OF-FREEDOM SYSTEM

6.1 The System

The systems is composed of the following blocks: A decoupling matrix, the power supplies, the plant, and the five controllers with the gain blocks.

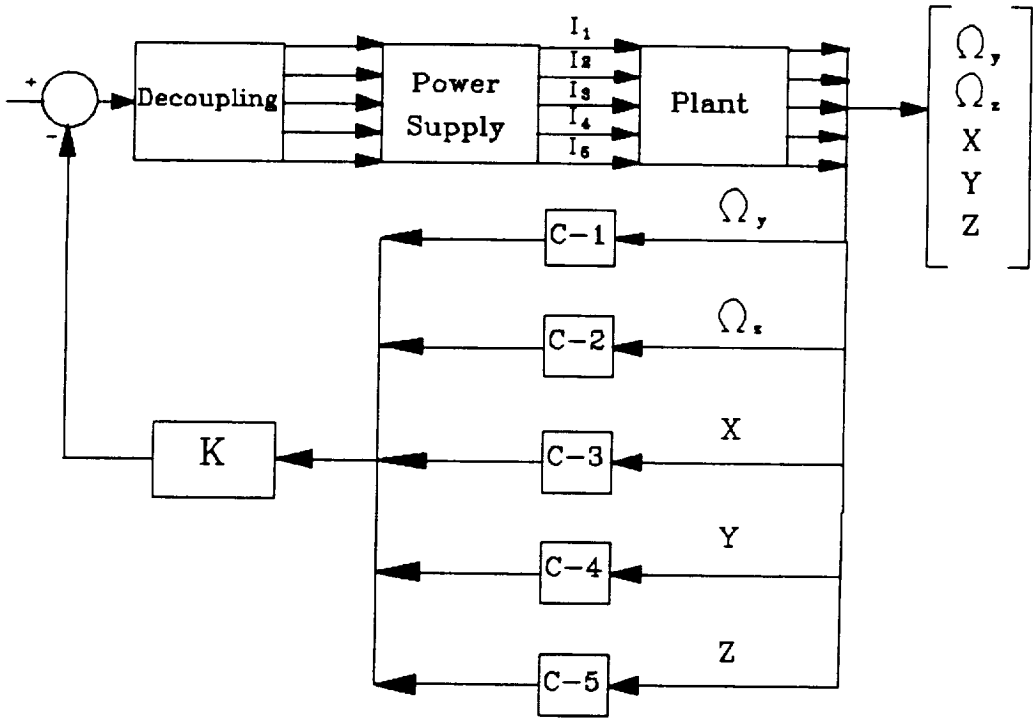

Figure 6.1.1 The five-degree-of-freedom system block diagram.

The decoupling matrix was created by computing the inverse of the magnetic field gradients matrix given in (Appendix A).

6.2 Power Supply:

The power supply governing differential equation takes the following form

$$V_i = I_i R_i + L_{ij}\frac{dI_j}{dt} + \ldots \qquad \text{where} \quad i = 1\ldots5 \;\; ; \;\; j = 1\ldots5 \qquad (6.2.1)$$

where V is the voltage, I is current, R is the resistance, and L is the inductance. If i = j, the result is self-inductance, but if i ≠ j, the outcome is mutual inductance L_m. Figure 6.2.1 shows the power supply diagram where the following equations apply

$$V_0 = R\,I + L\,\dot{I} + L_m \qquad (6.2.2)$$

$$V_0 = K(V_D - k\,I) \qquad (6.2.3)$$

$$V_j = V_{Dj} - kI_j \qquad (6.2.4)$$

Combining equations 6.2.2-4, the result is the following

$$[L]\,[\dot{I}] = [K\,V_D] - [K\,k]\,[I] - [R]\,[I] \qquad 6.2.5$$

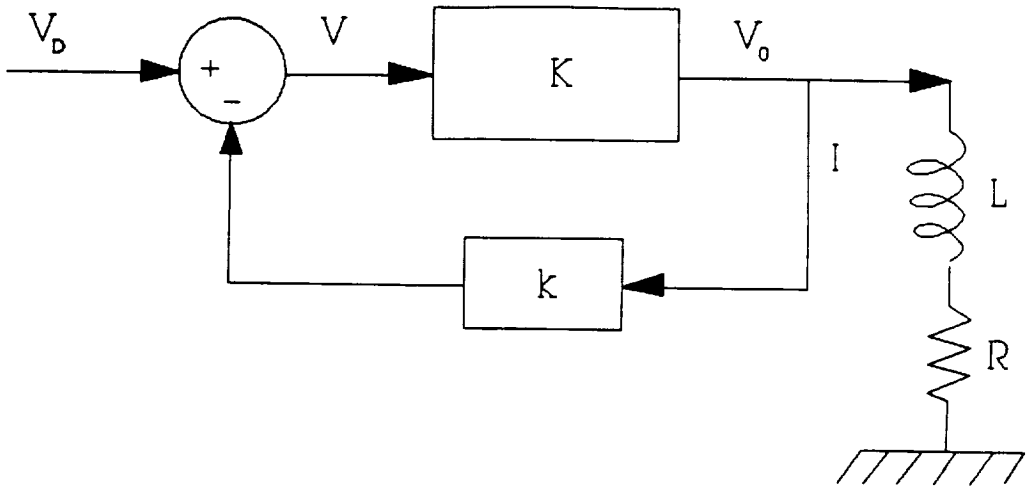

Figure 6.2.1 Power supply block diagram.

Following equation 6.2.5, the power supply matrices, for which values are given in Appendix A, have the following form

$$A = -\left[(K\,k + R)\,[\Psi]\,\left[\frac{1}{L}\right]\right] \tag{6.2.6}$$

where L is 5 x 5 matrix, (Kk + R) are constants and [Ψ] is an identity matrix.

The B matrix takes the following form

$$B = K\,[V_D] \tag{6.2.7}$$

The resulting matrices have the following dimensions

A is a 5 x 5 system dynamics matrix

B is a 5 x 5 input matrix

C is a 5 x 5 output matrix

D is a 5 x 5 matrix of zeros

The current distribution produced by the five electromagnets varies for each activated degree-of-freedom. The following graphs show which currents are produced for each degree-of-freedom. The table below represents the value of each of these figures.

I	Pitch	Yaw	X	Y	Z
1	-0.1611	-0.0000	0.1537	-0.0000	-0.0621
2	-0.0098	0.1352	-0.1249	0.0899	-0.0192
3	-0.1038	0.0835	0.0480	-0.1458	0.0503
4	-0.1038	-0.0835	0.0480	0.1458	0.0503
5	-0.0098	-0.1352	-0.1249	-0.0899	-0.0192

Table 6.2 Current values of the five degree-of-freedom system.

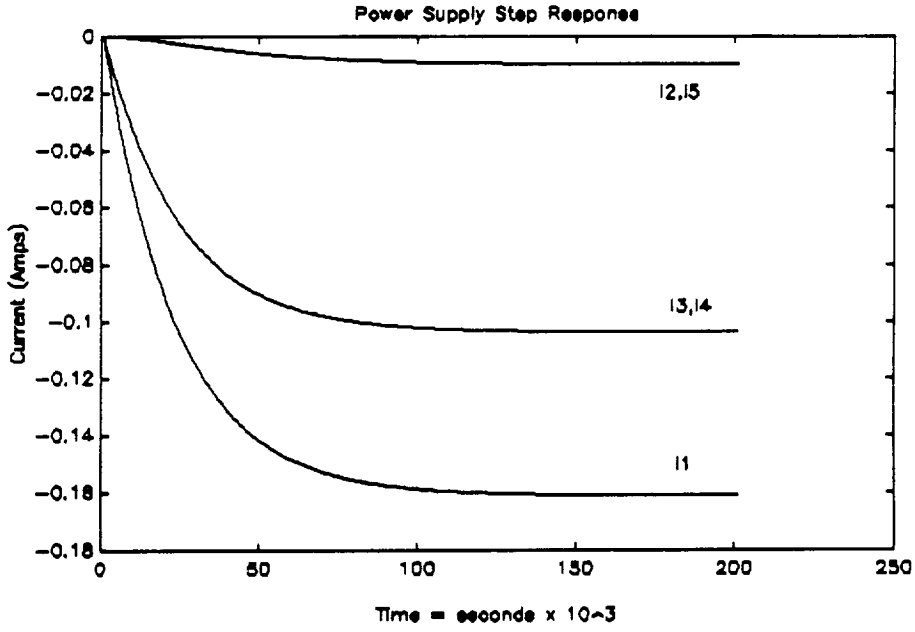

Figure 6.2.2 Power supply step response, "Pitch" degree-of-freedom.

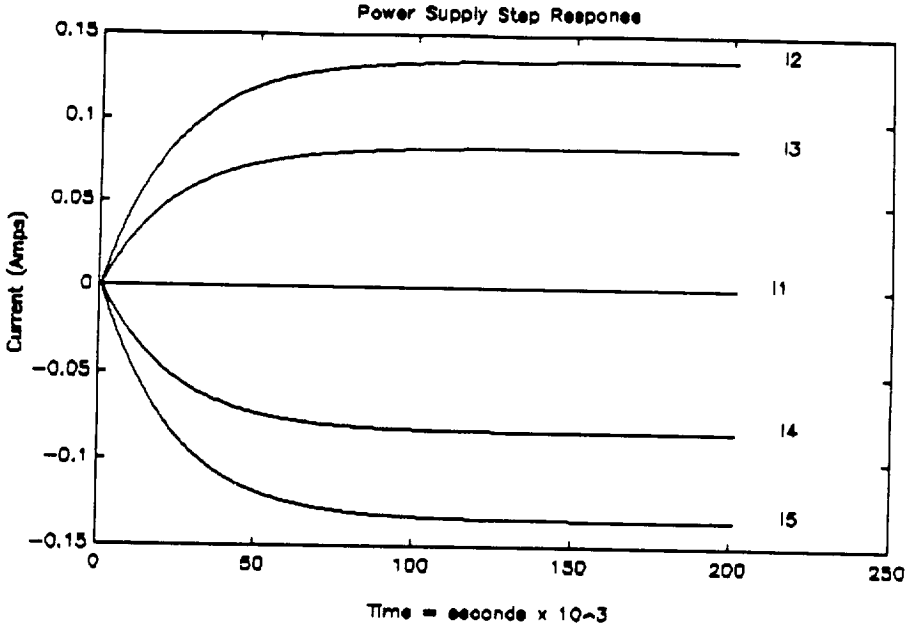

Figure 6.2.3 Power supply step response of yaw as the degree-of-freedom.

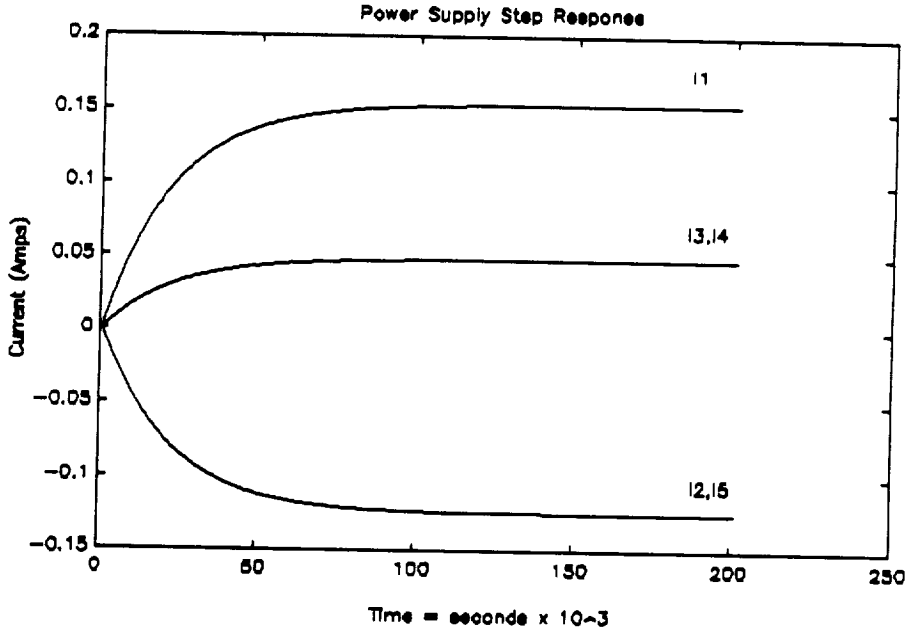

Figure 6.2.4 Power supply step response of X as the degree-of-freedom.

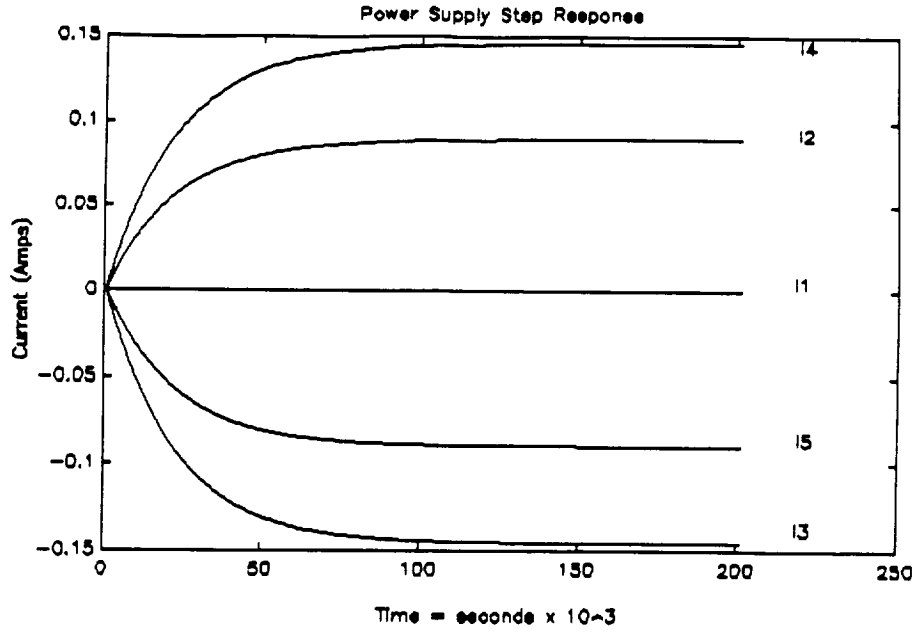

Figure 6.2.5 Power supply step response of Y as the degree-of-freedom.

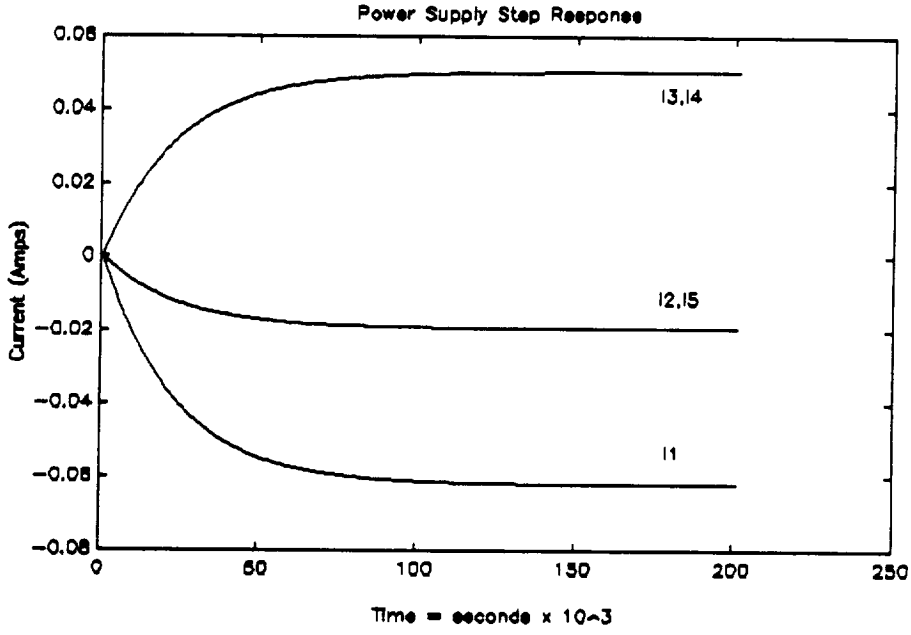

Figure 6.2.6 Power supply step response of Z as the degree-of-freedom.

6.3 The Plant:

The governing equations which lead to the development of the plant's matrices are given in Chapter 3. Those plant matrices were incorporated with the power supply matrices, and the five DPA matrices in order to produce the simulation of the entire system.

The derivation and numerical values of the plant's A, B, C, and D matrices are given in Appendix A. The following are the plant dimensions

A is a 10 x 10 system dynamics matrix

B is a 10 x 5 input matrix

C is a 10 x 10 output matrix

D is a 10 x 5 matrix of zeros

6.4 The Controllers:

A DPA controller transfer function was converted to a state-space form using MATLAB. Appending the state-space matrices of the DPA controller five times, state-space system matrices of the five controllers were created. The dimensions of these matrices are

A is 5 X 5

B is 5 X 5

C is 5 X 10

D is 5 X 10

As stated in Chapter 5, the numerical values of the DPA controller transfer function numerator and denominator were determined when the stability of the single-degree-of-freedom was accomplished.

Figure 6.4.1 shows a step response, which is identical for each of the five controllers.

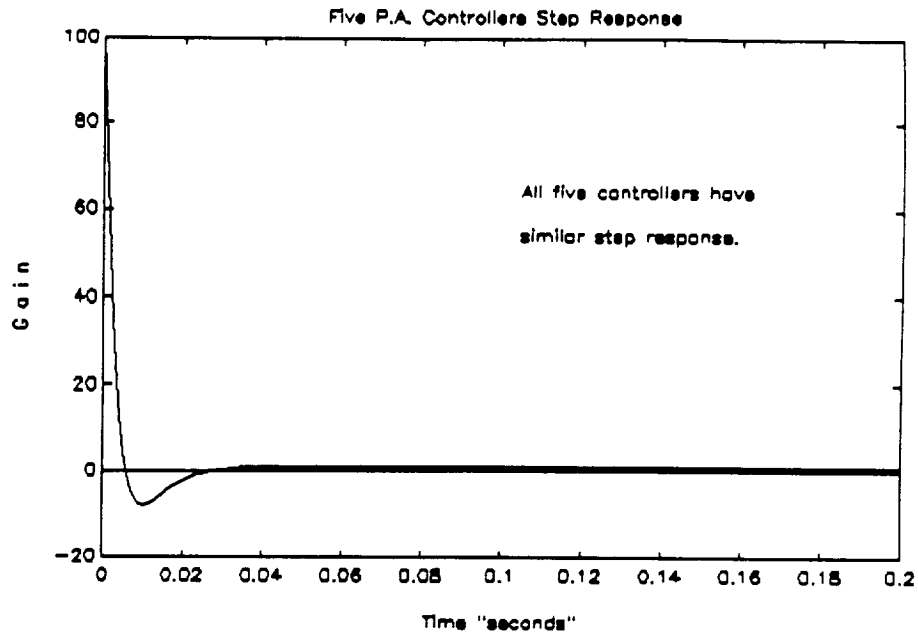

Figure 6.4.1 Step response of Dual Phase Advance controller.

6.5 Continuous-time Step Responses

The following step response graphs correspond to the above state-space system in a closed loop form. Each graph represents the behavior of the system when a certain degree-of-freedom is activated. To non dimensionalize the X degree-of-freedom, its values were divided by the length of the model which is equal to .3048 m.

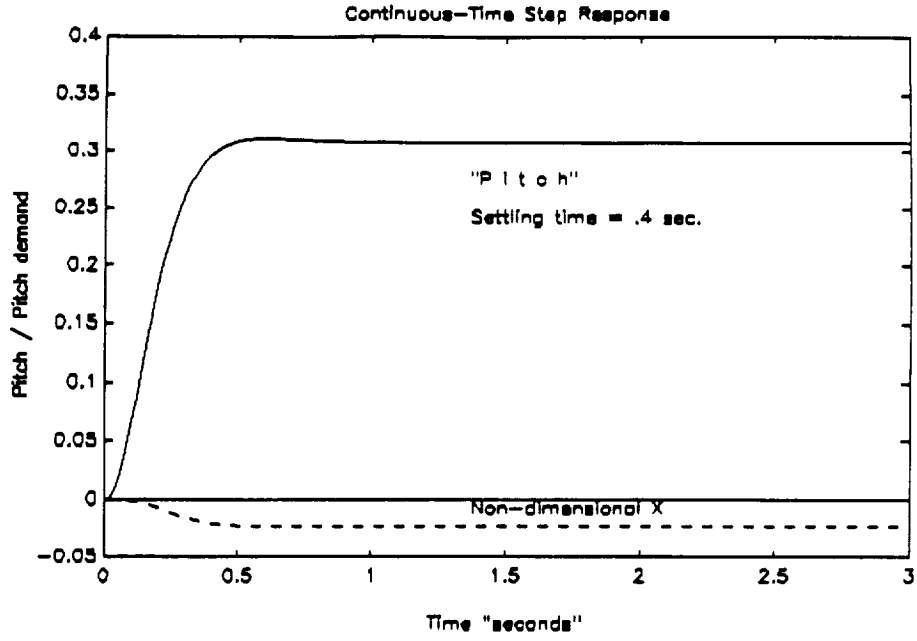

Figure 6.5.1 Continuous-time step response, "Pitch" degree-of-freedom.

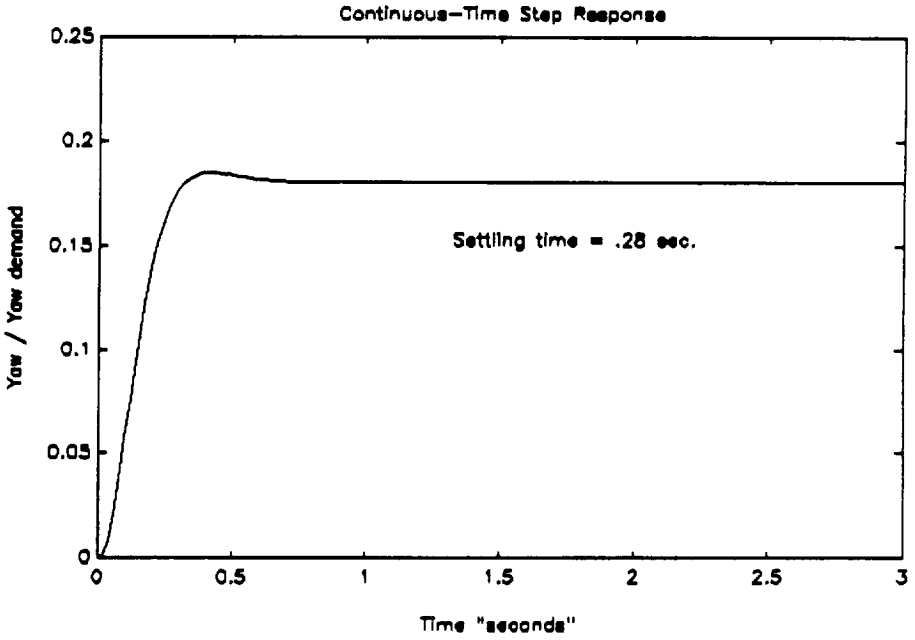

Figure 6.5.2 Continuous-time step response, Yaw degree-of-freedom.

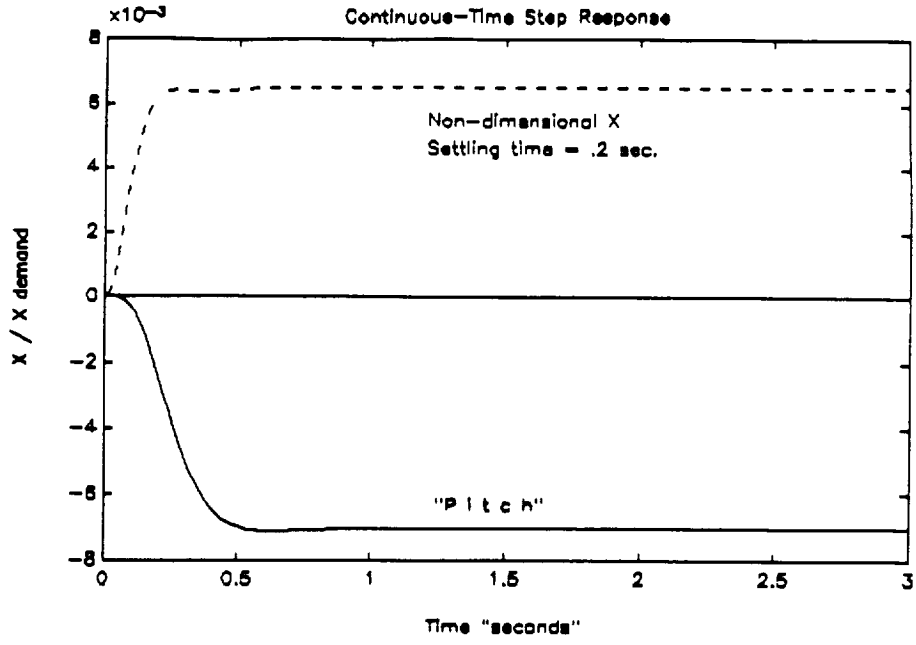

Figure 6.5.3 Continuous-time step response, Axial degree-of-freedom.

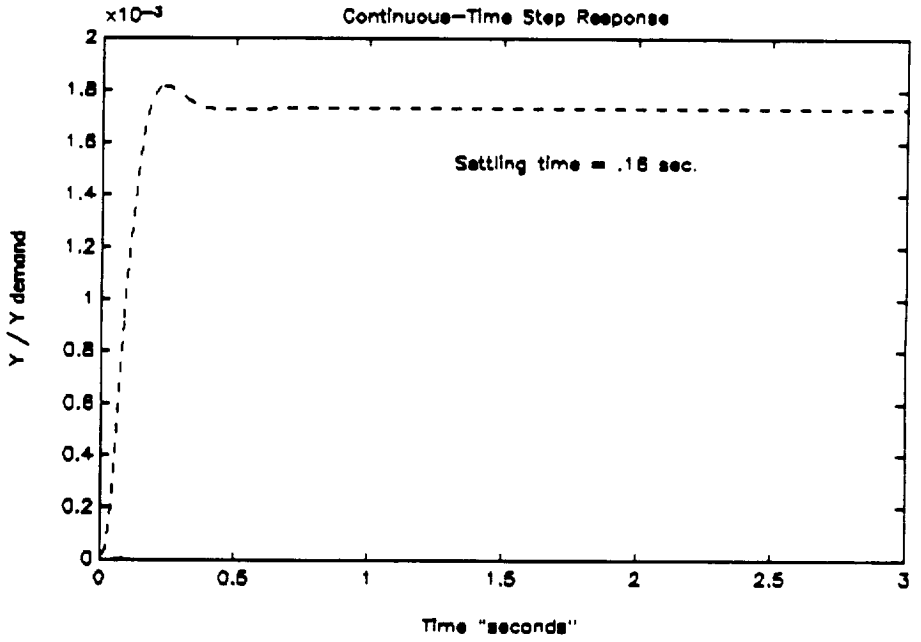

Figure 6.5.4 Continuous-time step response, Lateral degree-of-freedom.

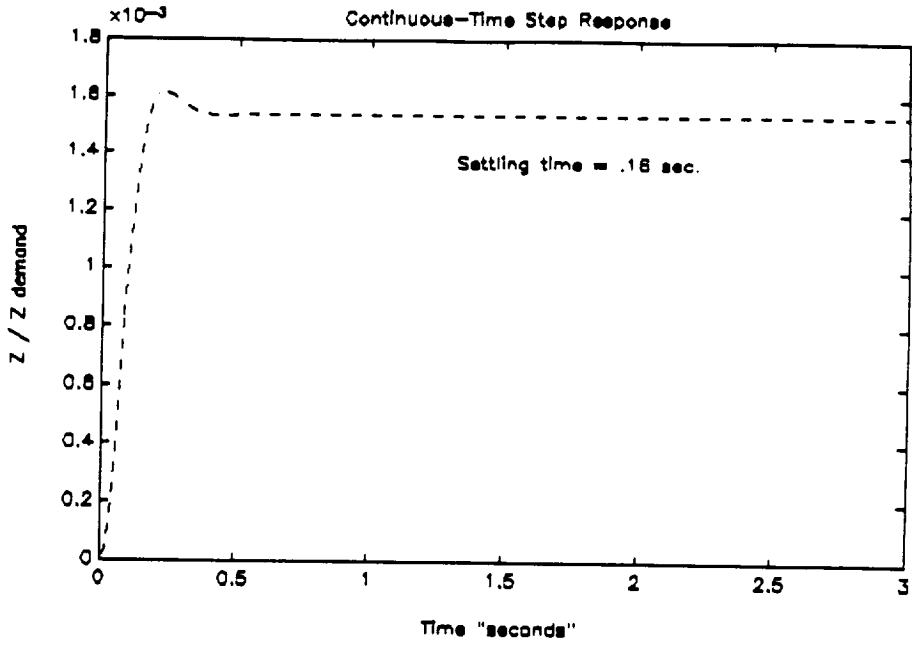

Figure 6.5.5 Continuous-time step response, Vertical degree-of-freedom.

6.6 Discrete-Time Step Responses:

To examine the behavior of the system, its state-space equations were converted to the discrete-time equations where a sample interval and a delay time was added. The sample interval and the delay time supposed to have an equal magnitude since all the degrees-of-freedom are sampled together to produce input. Once those degrees-of-freedom are processed and command output, the sampling procedure starts again without allowing any further delay time. The maximum value of the plant's eigenvalues (13.6986) was chosen since it represents the maximum frequency. The reciprocal of twice of this value (.0365) was taken to be the sample interval.

Testing the behavior of the system with different values of delay time, the discrete-time step responses remained virtually unchanged for low values, but for each degree-of-freedom, the

maximum value of delay time allowed before the system becomes unstable are given in the figures. Those values are at the critical point before instability occurs.

Comparing the step response curves Figures 6.6.1-5 before reaching the critical point of instability and Figures 6.5.1-5 for each degree of freedom, their behavior is virtually identical using the same gain value of each degree-of-freedom. This result shows that the system is well behaved and has a fast settling time of approximately .25 seconds which may increase or decrease by .01 seconds for each mode.

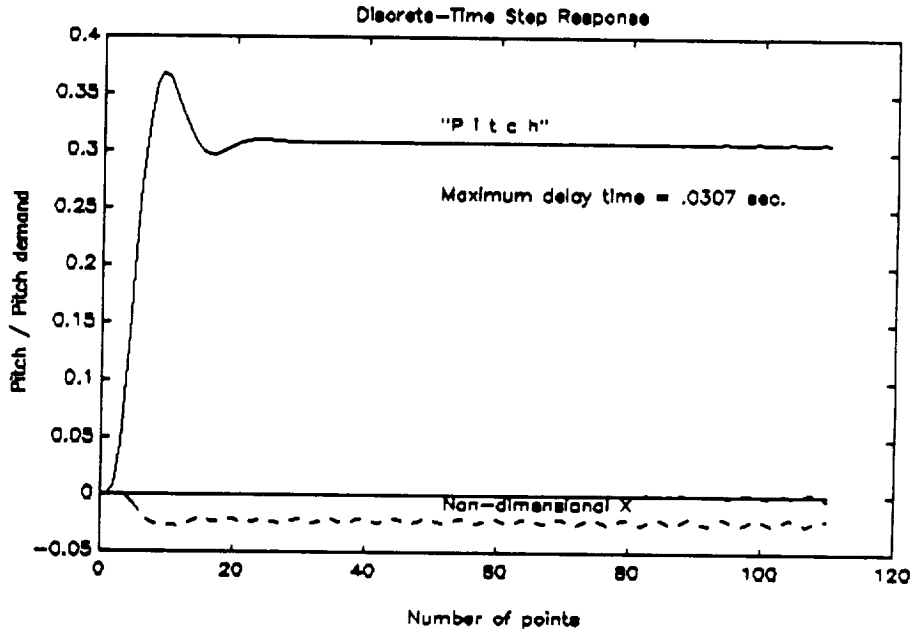

Figure 6.6.1 Discrete-time step response, "Pitch" degree-of-freedom.

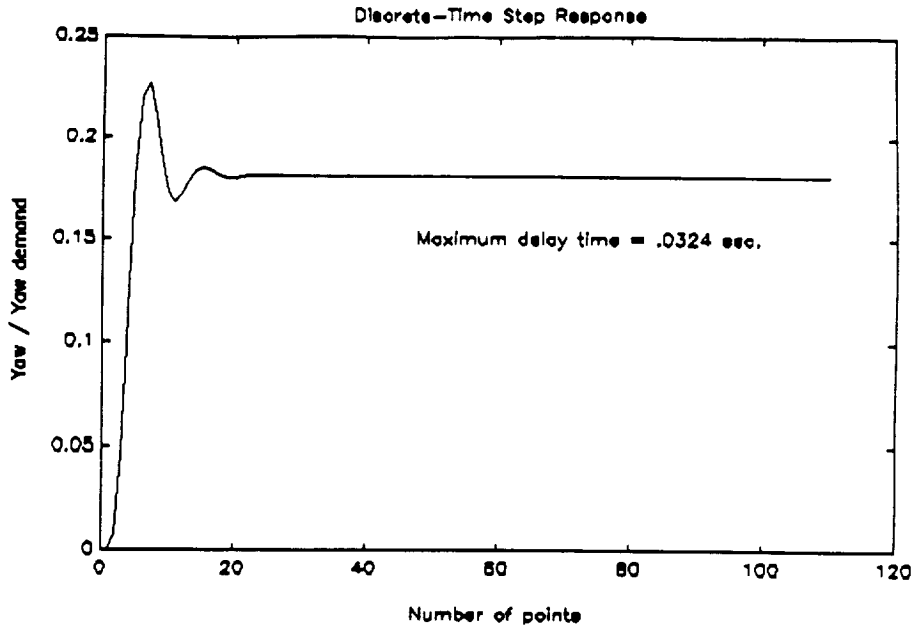

Figure 6.6.2 Discrete-time step response of Yaw degree-of-freedom.

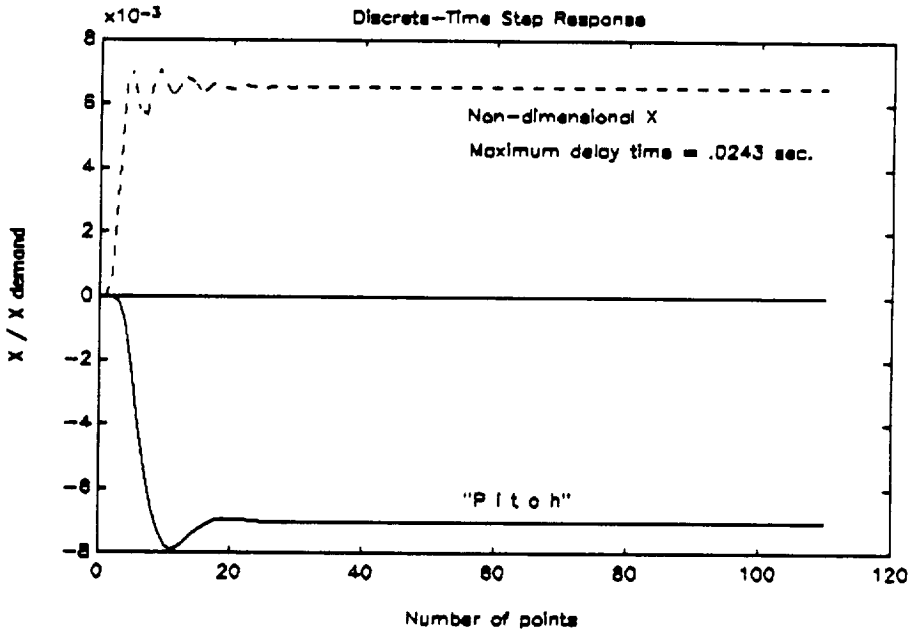

Figure 6.6.3 Discrete-time step response, Axial degree-of-freedom.

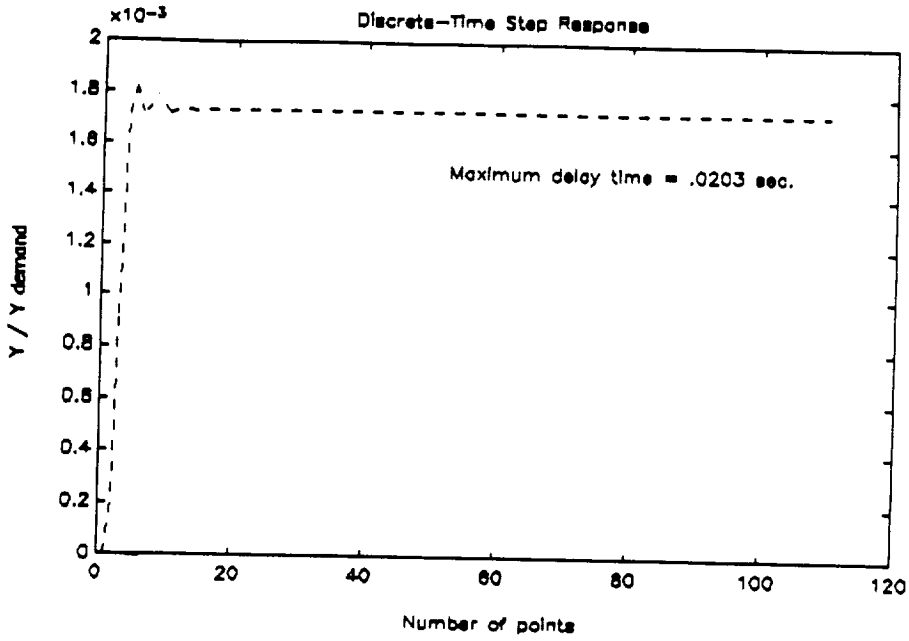

Figure 6.6.4 Discrete-time step response of the Lateral degree-of-freedom.

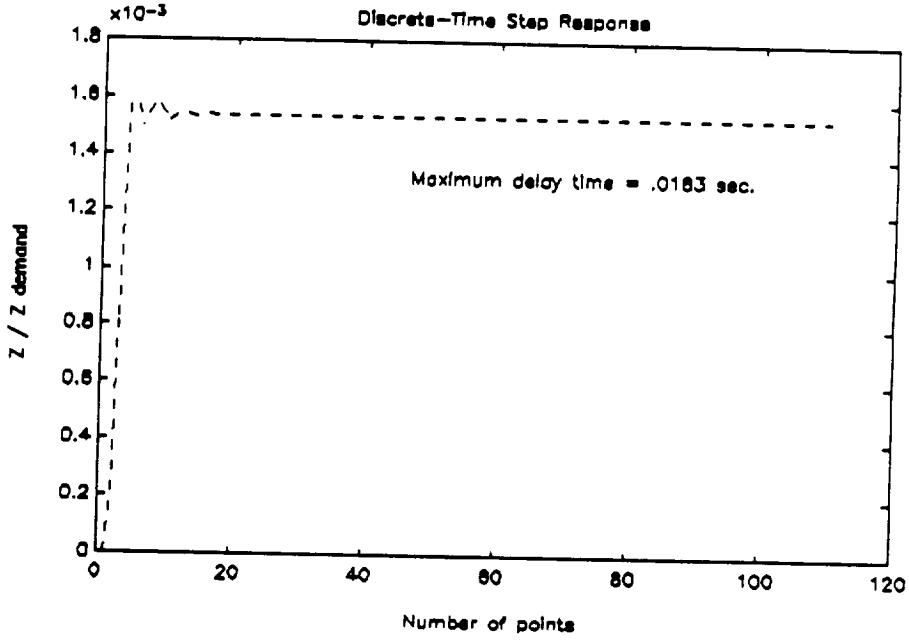

Figure 6.6.5 Discrete-time step response, Vertical degree-of-freedom.

CHAPTER 7

DISCUSSION

The focus of this thesis was the analysis of the five degree-of-freedom system simulation and testing the effect of white noise on the DPA and the PD controllers.

The single degree-of-freedom simulation program was executed separately for each of the two controllers. In the controllers subroutines, the output values were multiplied by .0001 for scaling purposes in order to be able to see its behavior in the graphics window created by the program. The previously determined gain values of both controllers were used since the five percent over-shoot criteria was adopted. The output data that included the white noise generated by the Gaussian function evaluated the noise performance (RMS) of both controllers. The values .145 and .6136 for the DPA an PD controllers respectively indicate that the DPA controller noise tolerance is about four times better. This data was also incorporated in a Fourier Transformation M-file to plot the power spectral density of both controllers where the resonant frequency of the controllers was approximated to about 10 Hz. Those spectral density plots do not present a smooth behavior of the noise due to insufficient number of points obtained from the simulation program. Considering the noise performance of both controllers, the DPA controller was chosen for the system while the PD controller is another very good alternative.

The resulting Dual Phase Advance controller was used in the single degree-of-freedom simulation in order to have an approximate value of the gain required to tune the overall five degree-of-freedom system. The gain value of this simulation (7) produced a good damping ratio of about .7 which is close to the target value of .707. Also, this gain value satisfied the criteria of achieving the five percent overshoot with the step response graphs.

Using this approximate gain value, the simulation of the five degree-of-freedom system

was executed in order to determine the gain matrix which provides a stable system that satisfies the step response criteria of five percent overshoot for each degree-of-freedom. The resulting system produced a fast settling time of about .24 seconds in addition to maintaining a damping ratio for each of the degrees-of-freedom of about .7 and above.

In order to determine the maximum value of the delay time required for each degree-of-freedom before they become unstable, a second order Pade Approximation was used with the closed-loop discrete system. A sampling time of .0365 was used which is the reciprocal of twice of the maximum frequency of the system. The resulting values of the delay time were between 50 and 75 percent of the sampling time which are a very good results.

Approximations and their effects

Approximations were made deriving the MSBS system governing equation. These equations are considered to be reasonable approximations of the non-linear system equations of the real MSBS where literature has also shown the linear approximation is a good representation of the system's dynamics (Ref. 4). For the bearing and the wind tunnel systems, these approximations apply well while they are operating on their equilibrium points. But during large position changes, these equations do not represent satisfactorily the dynamics away from the equilibrium point.

The availability of power supply is the most important factor for any MSBS system. It is possible to operate systems with their power supply capability is low, but when certain commands or loads are applied, great attention is required. This power supply limitation is not usually a problem for magnetic bearings since they only requires low amount of current, but for large gap MSBS, the power supply availability is a serious concern.

CHAPTER 8

CONCLUSIONS

The overall system is a feedback loop that contains a decoupling matrix, power supply, the plant, and five controllers. The values in each of the matrices in the above system were calculated using the system's parameters given in Appendix A.

Two controllers were tested to determine which is better suited for the system by generating white noise using the Gaussian equation with the single degree-of-freedom system. The output produced was used to plot the power spectral density of both controllers where a comparison was made between them. The outcome was that the two controllers have approximately similar resonant frequency but their gains were different.

The distinguishing result of both controllers was the noise performance (RMS), where the DPA controller has better tolerance to noise than the PD controller and this was the dominant condition of choosing the controller of the system. In addition to this result, the single degree-of-freedom system step responses were examined with both controllers where they both showed a rapid settling time and an over- shoot which met the criteria value of five percent error and lower. Due to these results, the DPA controller was chosen for this system.

With the determination of the controller type, a single degree-of-freedom transfer function of the yaw mode was acquired using the overall system's matrix (Appendix A). The new resulting system's transfer function was used to determine the location of the poles and zeros of the DPA controller by using root-locus plot. Different locations of these poles and zeros were examined until the appropriate root-locus plot that shows stability with acceptable amount of gain was achieved. This resulting gain was used to obtain the step response of the system.

After determining the desired location of the poles and zeros of the DPA controller, this

controller was appended four times in order for the five resulting controllers be incorporated in the overall five degree-of-freedom system.

The basic system provides five degree-of-freedom control of a suspended cylinder that contains a core composed of permanent magnet material. The magnetization vector is along the horizontal axis of the cylinder. This system uses five elecrtomagnets which is the minimum configuration for a five degree-of-freedom control. The highest frequency open-loop mode is the compass-needle mode that result from the magnetization vector trying to align itself with the applied field and it is caused by the presence of B_x. Since those high frequencies are caused by B_x and since B_x is uncontrolled with five-coil, increasing the number of coils might make it possible to independently control B_x and, therefore, control the highest open-loop frequencies.

This system is a multi-input multi-output system, some of the modes in this system are coupled, therefore, simulation of the system was performed where the strategy to control each degree of freedom was adopted. Using MATLAB, the gain matrix (Appendix A) produced a stable system by using each degree-of-freedom separately starting with the vertical followed by the lateral, yaw, the axial, and pitch. The order of difficulty to stabilize each of those degrees-of-freedom is different, therefore the order of simplicity to achieve stability was followed. The continuous step response plots of the five modes show that the system is well behaved since the overshoot of all of the degrees-of-freedom fell bellow the criteria of five percent error value and has a quick settling time. Discrete-time step responses of all the degrees-of-freedom were also produced and showed promising results as the above continuous step responses.

After examining the results produced by the simulations and observing the behavior of the system, it is concluded that the overall system is well behaved and exhibits a very good stability.

REFERENCES

1. Holmes, F. T.: Axial Magnetic Suspension. Review of Scientific Instruments, Vol 8, November 1937.

2. Tournier, Marcel; and Laurenceau, P.: Suspension Magnetique d'une Maquette en Soufflerie. (Magnetic Suspension of a Model in a Wind Tunnel.) La Recherche Aeronautique, No. 59, July - August 1957.

3. Boyden, R. P.: A Review of Magnetic Suspension and Balance Systems. AIAA 15th Aerodynamic Testing Conference, San Diego, California, May 18-20, 1988.

4. Tuttle, Marie H.; kilgore, Robert A.; and Boyden, Richmond P.: Magnetic Suspension and Balance Systems. A selected, Annotated Bibliography. NASA Technical Memorandum 84661, February 1988.

5. Kilgore, William, A.: Comparison of Digital Controllers Used in Magnetic Suspension and Balance Systems. NASA Contractor Report 182087, December 1989.

6. Britcher, Colin, P.: Technical Background for a Demonstration Magnetic Levitation System. Department of Mechanical Engineering and Mechanics, Old Dominion University, Norfolk, VA. Grant NAG1-716, May 1987.

7. Groom, Nelson, J.: Analytical Model of Five Degree of Freedom Magnetic Suspension and Positioning System. NASA Technical memorandum 100671, March 1989.

8. Britcher, Colin, P.; Groom, Nelson, J.: Stability Considerations for Magnetic Suspension Systems Using Electromagnets Mounted in a Planar Array. NASA Conference Publication 10066, Part 1.

9. Groom, Nelson, J.; Britcher, Colin, P.: Open-Loop Characteristics of Magnetic Suspension Systems With Electromagnets Mounted in a Planar Array. NASA TP-3229, May 1992.

10. Takahashi, Y.; Rabins, M. J.; Auslander, D. M.: Control and Dynamic Systems. Addison-Wesley Publishing, Co., 1970.

11. Maciejowski, J. M.: Multivariable Feedback Design. Addison-Wesley Publishing, Ltd., 1989.

12. Buckingham, M. J.: Noise in Electronic Devices and Systems. John Wiley & Sons, Inc., 1983.

13. Lewis, T. G.: Distribution Sampling for Computer Simulation. Heath and Company, 1975.

14. MATLAB. The MathWorks, Inc.

15. Jayawant, B. V.: Electromagnetic Levitation and Suspension Techniques. Edward Arnold (Publishers) Ltd., 1981.

16. Parker, D. and Britcher, C. P.: Progress Toward Extreme Attitude Testing with Magnetic Suspension and Balance Systems. AIAA 15th Aerodynamic Testing Conference, San Diego, California, May 18-20, 1988.

17. Beaussler, J. nd Zakneim, J.: Telemetrie Multivoies pour Maquettes en Suspension Magnetique. (Multichannel Telemetering Device for Magnetically Suspended Models) Presented at the Colloquium on the Properties and behavior of Electronic Components and Assemblies Submitted to Strong Acceleration. Saint-Louis, France. October 1968.

18. Franklin, G. F.; Powel, J. D.; and Emami-Naeini, Abbas: Feedback Control of Dynamic Systems. Addison-Wesley Publishing Company Inc., Massachusetts, 1986.

19. Matsuda, R.; Nakagawa, M.; and Yamada, I.: Multi Input-Output Control of a Magnetically Suspended Linear Guide. IEEE Transactions on Magnetics, MAG-20, No. 5, September 1984.

20. Hornbeck, Robert W.: Numerical Methods. Prentice-Hall, Inc., New Jersey, USA, 1975.

21. Microsoft QuickBASIC Version 4.5. Microsoft Corporation 1988.

22. Britcher, C. P.: User Guide for the Digital Control System of the NASA/Langley Research Center's 13-inch Magnetic Suspension and Balance System. Old Dominion University Research Foundation, NASA CR 178210, March 1987.

23. Sawada, Hideo; Kanda, Hiroshi; and Suenaga, Hisashi: Aposition and Attitude Sensing Camera in NAL's MSBS. MSBS Newsletter published by the Experimental Techniques Branch, NASA Langley Research Center, No. 4, January 1988.

24. Bradley, Fennimore N.: Materials for Magnetic Functions. Hayden Book Company, Inc., 1971.

APPENDIX A

The development of the plant state-space matrices has the following procedure:

Using the small angle assumptions and assuming that the magnetization is along the long (x) axis of the core, that is

$$[\bar{M}] = [M_{\bar{x}} \quad 0 \quad 0]$$

Assuming Θ_x is zero, the torque and force equations reduce to

$$\bar{T}_y = (vol)\, M_{\bar{x}} (-\theta_y B_x - B_z)$$

$$\bar{T}_z = (vol)\, M_{\bar{x}} (-\theta_z B_x + B_y)$$

$$\bar{F}_x = (vol)\, M_{\bar{x}} (B_{xx} + \theta_z B_{xy} - \theta_y B_{xz} + \theta_z B_{yx} - \theta_y B_{zx})$$

$$\bar{F}_y = (vol)\, M_{\bar{x}} (-\theta_z B_{xx} + B_{yx} + \theta_z B_{yy} + \theta_y B_{yz})$$

$$\bar{F}_z = (vol)\, M_{\bar{x}} (\theta_y B_{xx} + B_{zx} + \theta_z B_{zy} - \theta_y B_{zz})$$

Using the electromagnet specifications (Ref. 9)

Inner radius	=	0.173 m
Outer radius	=	0.386 m
Depth	=	0.493 m
Location radius	=	0.7 m
Maximum current density	=	1535.87 A/cm^2
Datum orientation	=	Positive $\bar{x}$ axis vertically over coil 1

-the field and field gradient contributions for the full design current

	COIL				
	1	2	3	4	5
B_x	0.0216	0.0067	-0.0175	-0.0175	0.0067
B_y	0	0.0206	0.0127	-0.0127	-0.0206
B_z	-0.0198	-0.0198	-0.0198	-0.0198	-0.0198
B_{xx}	0.0092	-0.0269	-0.0046	-0.0046	-0.0269
B_{xy}	0	0.0118	-0.0191	0.0191	-0.0118
B_{xz}	-0.0497	-0.0152	0.04	0.04	-0.0152
B_{yy}	-0.0306	0.0054	-0.017	-0.017	0.0054
B_{yz}	0	-0.0472	-0.029	0.029	0.0472

Table A.1 Field gradients contributions values.

The model specifications are (Ref. 9)

Magnet length	=	0.3048 m
Magnet diameter	=	0.1016 m
Magnetization	=	954930 A/m/m (1.2 Tesla)
Total mass	=	23.11 kg
Moment of inertia	=	0.6 kg m^2

Using the expression for torque and force developed earlier, this means that

$B_{xx} = B_{yx} = B_{xy} = B_z = B_y = 0$ and $F_x = F_y = T_y = T_z = 0$. This results in

$$\bar{T}_{y\theta_y} = -(vol)\, M_{\bar{x}}\, B_x \qquad \bar{T}_{y\theta_z} = 0$$

$$\bar{T}_{yx} = -(vol)\, M_{\bar{x}}\, B_{zx} \qquad \bar{T}_{yy} = -(vol)\, M_{\bar{x}}\, B_{zy}$$

$$\bar{T}_{yz} = -(vol)\, M_{\bar{x}}\, B_{zz} \qquad \bar{T}_{z\theta_y} = 0$$

$$\bar{T}_{z\theta_z} = -(vol)\, M_{\bar{x}}\, B_x \qquad \bar{T}_{zx} = 0$$

$$\bar{T}_{zy} = (vol)\, M_{\bar{x}}\, B_{yy} \qquad \bar{T}_{zz} = (vol)\, M_{\bar{x}}\, B_{yz}$$

$$\bar{F}_{x\theta_y} = -(vol)\, M_{\bar{x}}\, B_{xz} \qquad \bar{F}_{x\theta_z} = 0$$

$$\bar{F}_{xx} = (vol)\, M_{\bar{x}}\, B_{(xx)x} \qquad \bar{F}_{xy} = (vol)\, M_{\bar{x}}\, B_{(xx)y}$$

$$\bar{F}_{xz} = (vol)\, M_{\bar{x}}\, B_{(xx)z} \qquad \bar{F}_{y\theta_x} = -(vol)\, M_{\bar{x}}\, B_{yz}$$

$$\bar{F}_{y\theta_z} = (vol)\, M_{\bar{x}}\, B_{yy} \qquad \bar{F}_{yx} = (vol)\, M_{\bar{x}}\, B_{(yx)x}$$

$$\bar{F}_{yy} = (vol)\, M_{\bar{x}}\, B_{(yx)y} \qquad \bar{F}_{yz} = (vol)\, M_{\bar{x}}\, B_{(yx)z}$$

$$\bar{F}_{z\theta_y} = -(vol)\, M_{\bar{x}}\, B_{zz} \qquad \bar{F}_{z\theta_z} = (vol)\, M_{\bar{x}}\, B_{zy}$$

$$\bar{F}_{zx} = (vol)\, M_{\bar{x}}\, B_{(zx)x} \qquad \bar{F}_{zy} = (vol)\, M_{\bar{x}}\, B_{(zx)y}$$

$$\bar{F}_{zz} = (vol)\, M_{\bar{x}}\, B_{(zx)z}$$

Due to symmetry, for a five coil configuration

$B_{yz} = B_{zy} = 0$ $\quad B_{yy} = -B_{zz} \approx 0$ $\quad B_{(yx)z} = B_{(xy)z} = 0$ $\quad B_{(xx)y} = 0$

$B_{(zx)y} = B_{(zz)y} = 0$ $\quad B_{(xx)z} \approx 0$ $\quad B_{(xx)x} = B_{(zz)x} \approx 0$ $\quad B_{(yx)x} = B_{(xy)x} = 0$

To obtain some of the above B_{yz} and $B_{(yx)z}$ relationships, Maxwell's equations were used. The non-zero terms are B_{zx}, $B_{(xx)x}$, $B_{(yx)y}$, B_x, and $B_{(xx)z}$. The related non-zero elements of the A matrix are

$$\bar{T}_{y\theta_y} = -(vol)\, M_{\bar{x}}\, B_x \qquad \bar{T}_{yx} = -(vol)\, M_{\bar{x}}\, B_{xz}$$

$$\bar{T}_{z\theta_z} = -(vol)\, M_{\bar{x}}\, B_x \qquad \bar{F}_{x\theta_y} = -(vol)\, M_{\bar{x}}\, B_{xz}$$

$$\bar{F}_{xx} = (vol)\, M_{\bar{x}}\, B_{(xx)x} \qquad \bar{F}_{yy} = (vol)\, M_{\bar{x}}\, B_{(yx)y}$$

$$\bar{F}_{zz} = (vol)\, M_{\bar{x}}\, B_{(zx)z}$$

Using the values of the above coefficients, the resulting A matrix is

$$A = \begin{bmatrix}
0 & 0 & 165.424 & 0 & 0 & 0 & 0 & -378.359 & 0 & 0 \\
0 & 0 & 0 & 165.424 & 0 & 0 & 0 & 0 & 0 & 0 \\
1 & 0 & 0 & 0 & 0 & 0 & 0 & 0 & 0 & 0 \\
0 & 1 & 0 & 0 & 0 & 0 & 0 & 0 & 0 & 0 \\
0 & 0 & -9.8225 & 0 & 0 & 0 & 0 & 18.858 & 0 & 0 \\
0 & 0 & 0 & 0 & 0 & 0 & 0 & 0 & 6.279 & 0 \\
0 & 0 & 0 & 0 & 0 & 0 & 0 & 0 & 0 & -25.314 \\
0 & 0 & 0 & 0 & 1 & 0 & 0 & 0 & 0 & 0 \\
0 & 0 & 0 & 0 & 0 & 1 & 0 & 0 & 0 & 0 \\
0 & 0 & 0 & 0 & 0 & 0 & 1 & 0 & 0 & 0
\end{bmatrix}$$

The resulting B matrix is

$$B = \begin{bmatrix} 77.8679 & 77.8679 & 77.8679 & 77.8679 & 77.8679 \\ 0 & 81.014 & 49.9455 & -49.9455 & -81.014 \\ 0 & 0 & 0 & 0 & 0 \\ 0 & 0 & 0 & 0 & 0 \\ .9394 & -2.7466 & -.4697 & -.4697 & -2.7466 \\ 0 & 1.2048 & -1.9502 & 1.9502 & -1.2048 \\ -5.0746 & -1.552 & 4.0842 & 4.0842 & -1.552 \\ 0 & 0 & 0 & 0 & 0 \\ 0 & 0 & 0 & 0 & 0 \\ 0 & 0 & 0 & 0 & 0 \end{bmatrix}$$

$$C = \begin{bmatrix} 1 & 0 & 0 & 0 & 0 & 0 & 0 & 0 & 0 & 0 \\ 0 & 1 & 0 & 0 & 0 & 0 & 0 & 0 & 0 & 0 \\ 0 & 0 & 1 & 0 & 0 & 0 & 0 & 0 & 0 & 0 \\ 0 & 0 & 0 & 1 & 0 & 0 & 0 & 0 & 0 & 0 \\ 0 & 0 & 0 & 0 & 1 & 0 & 0 & 0 & 0 & 0 \\ 0 & 0 & 0 & 0 & 0 & 1 & 0 & 0 & 0 & 0 \\ 0 & 0 & 0 & 0 & 0 & 0 & 1 & 0 & 0 & 0 \\ 0 & 0 & 0 & 0 & 0 & 0 & 0 & 1 & 0 & 0 \\ 0 & 0 & 0 & 0 & 0 & 0 & 0 & 0 & 1 & 0 \\ 0 & 0 & 0 & 0 & 0 & 0 & 0 & 0 & 0 & 1 \end{bmatrix}$$

$$D = \begin{bmatrix} 0 & 0 & 0 & 0 & 0 \\ 0 & 0 & 0 & 0 & 0 \\ 0 & 0 & 0 & 0 & 0 \\ 0 & 0 & 0 & 0 & 0 \\ 0 & 0 & 0 & 0 & 0 \\ 0 & 0 & 0 & 0 & 0 \\ 0 & 0 & 0 & 0 & 0 \\ 0 & 0 & 0 & 0 & 0 \\ 0 & 0 & 0 & 0 & 0 \\ 0 & 0 & 0 & 0 & 0 \end{bmatrix}$$

The power supply

Factoring terms in equation 6.2.5, the result is

$$I(R + LD + kK) = KV_D$$

in a matrix form, the above equation becomes

$$[L_{ij}][\dot{I}] = -[(R + kK)][I_i] + [K]V_{D_i}$$

To produce the A and B matrix, [(R + kK)] and [K] were multiplied by the inverse of the inductance matrix respectively.

The inductance matrix is

$$L = \begin{bmatrix} 2.9668 & 0.1082 & 0.0247 & 0.0247 & 0.1082 \\ 0.1082 & 2.9668 & 0.1082 & 0.0247 & 0.0247 \\ 0.0247 & 0.1082 & 2.9668 & 0.1082 & 0.0247 \\ 0.0247 & 0.0247 & 0.1082 & 2.9668 & 0.1082 \\ 0.1082 & 0.0247 & 0.0247 & 0.1082 & 2.9668 \end{bmatrix}$$

$$A = \begin{bmatrix} -43.9375 & 1.5759 & 0.2849 & 0.2849 & 1.5759 \\ 1.5759 & -43.9375 & 1.5759 & 0.2849 & 0.2849 \\ 0.2849 & 1.5759 & -43.9375 & 1.5759 & .2849 \\ 0.2849 & .2849 & 1.5759 & -43.9375 & 1.5759 \\ 1.5759 & 0.2849 & 0.2849 & 1.5759 & -43.9375 \end{bmatrix}$$

$$B = \begin{bmatrix} .3380 & -0.0121 & -0.0022 & -0.0022 & -0.0121 \\ -.0121 & .3380 & -0.0121 & -0.0022 & -0.0022 \\ -.0022 & -.0121 & .3380 & -0.0121 & -0.0022 \\ -0.0022 & -.0022 & -.0121 & .3380 & -0.0121 \\ -0.0121 & -0.0022 & -0.0022 & -0.0121 & 0.3380 \end{bmatrix}$$

The decoupling matrix was evaluated by taking the inverse of the field gradients matrix and is equal to

$$\begin{bmatrix} -20.95 & 0.0 & 19.985 & 0.0 & -8.074 \\ -1.27 & 17.58 & -16.24 & 11.69 & -2.498 \\ -13.5 & 10.86 & 6.245 & -18.96 & 6.535 \\ -13.5 & -10.86 & 6.245 & 18.96 & 6.535 \\ -1.27 & -17.58 & -16.238 & -11.69 & -2.498 \end{bmatrix}$$

The B matrix is multiplied by the decoupling matrix to produce the following

$$BC = \begin{bmatrix} -6.9918 & 0.00 & 7.1208 & -0.00 & -2.6968 \\ 0.0194 & 5.8714 & -5.7841 & 4.1640 & -0.8345 \\ -4.3354 & 3.6273 & 2.2237 & -6.7531 & 2.1829 \\ -4.3354 & -3.6273 & 2.2237 & 6.7531 & 2.1829 \\ 0.0194 & -5.8714 & -5.7841 & -4.1640 & -0.8345 \end{bmatrix}$$

The above BC matrix is used as the B matrix since it includes decoupling.

$$C = \begin{bmatrix} 1 & 0 & 0 & 0 & 0 \\ 0 & 1 & 0 & 0 & 0 \\ 0 & 0 & 1 & 0 & 0 \\ 0 & 0 & 0 & 1 & 0 \\ 0 & 0 & 0 & 0 & 1 \end{bmatrix} \qquad D = \begin{bmatrix} 0 & 0 & 0 & 0 & 0 \\ 0 & 0 & 0 & 0 & 0 \\ 0 & 0 & 0 & 0 & 0 \\ 0 & 0 & 0 & 0 & 0 \\ 0 & 0 & 0 & 0 & 0 \end{bmatrix}$$

The five Dual Phase Advance controllers matrices

$$A = 10^4 \begin{bmatrix} -.044 & -4.84 & 0 & 0 & 0 & 0 & 0 & 0 & 0 & 0 \\ .0001 & 0 & 0 & 0 & 0 & 0 & 0 & 0 & 0 & 0 \\ 0 & 0 & -.044 & -4.84 & 0 & 0 & 0 & 0 & 0 & 0 \\ 0 & 0 & .0001 & 0 & 0 & 0 & 0 & 0 & 0 & 0 \\ 0 & 0 & 0 & 0 & -.044 & -4.84 & 0 & 0 & 0 & 0 \\ 0 & 0 & 0 & 0 & .0001 & 0 & 0 & 0 & 0 & 0 \\ 0 & 0 & 0 & 0 & 0 & 0 & -.044 & -4.84 & 0 & 0 \\ 0 & 0 & 0 & 0 & 0 & 0 & .0001 & 0 & 0 & 0 \\ 0 & 0 & 0 & 0 & 0 & 0 & 0 & 0 & -.044 & -4.84 \\ 0 & 0 & 0 & 0 & 0 & 0 & 0 & 0 & .0001 & 0 \end{bmatrix}$$

$$B = \begin{bmatrix} 0 & 0 & 1 & 0 & 0 & 0 & 0 & 0 & 0 & 0 \\ 0 & 0 & 0 & 0 & 0 & 0 & 0 & 0 & 0 & 0 \\ 0 & 0 & 0 & 1 & 0 & 0 & 0 & 0 & 0 & 0 \\ 0 & 0 & 0 & 0 & 0 & 0 & 0 & 0 & 0 & 0 \\ 0 & 0 & 0 & 0 & 0 & 0 & 0 & 1 & 0 & 0 \\ 0 & 0 & 0 & 0 & 0 & 0 & 0 & 0 & 0 & 0 \\ 0 & 0 & 0 & 0 & 0 & 0 & 0 & 0 & 1 & 0 \\ 0 & 0 & 0 & 0 & 0 & 0 & 0 & 0 & 0 & 0 \\ 0 & 0 & 0 & 0 & 0 & 0 & 0 & 0 & 0 & 1 \\ 0 & 0 & 0 & 0 & 0 & 0 & 0 & 0 & 0 & 0 \end{bmatrix}$$

$$C = 10^6 \begin{bmatrix} -.04 & -4.79 & 0 & 0 & 0 & 0 & 0 & 0 & 0 & 0 \\ 0 & 0 & -.04 & -4.79 & 0 & 0 & 0 & 0 & 0 & 0 \\ 0 & 0 & 0 & 0 & -.04 & -4.79 & 0 & 0 & 0 & 0 \\ 0 & 0 & 0 & 0 & 0 & 0 & -.04 & -4.79 & 0 & 0 \\ 0 & 0 & 0 & 0 & 0 & 0 & 0 & 0 & -.04 & -4.79 \end{bmatrix}$$

$$D = \begin{bmatrix} 0 & 0 & 100 & 0 & 0 & 0 & 0 & 0 & 0 & 0 \\ 0 & 0 & 0 & 100 & 0 & 0 & 0 & 0 & 0 & 0 \\ 0 & 0 & 0 & 0 & 0 & 0 & 0 & 100 & 0 & 0 \\ 0 & 0 & 0 & 0 & 0 & 0 & 0 & 0 & 100 & 0 \\ 0 & 0 & 0 & 0 & 0 & 0 & 0 & 0 & 0 & 100 \end{bmatrix}$$

The five degree-of-freedom gain matrix

The following gain matrix was formed by restricting the step response of each of the five degrees-of-freedom to five percent overshoot.

$$Gain = \begin{bmatrix} 9 & 0 & 0 & 0 & 0 \\ 0 & 11 & 0 & 0 & 0 \\ 0 & 0 & 572 & 0 & 0 \\ 0 & 0 & 0 & 586 & 0 \\ 0 & 0 & 0 & 0 & 618 \end{bmatrix}$$

APPENDIX B

SINGLE DEGREE-OF-FREEDOM M FILES

The "MATLAB" M files below evaluate the numerator and denominator of single degree of freedom system combined with the Dual Phase Advance controller to produce the compensated system transfer function. The files may be named as (filename.m).

To achieve a stable system, the poles and zeros of the controller were examined in different locations. Once those value were produced, a root-locus graph was plotted and the value of gain that produces stability was determined. For this purpose, the root-locus M file was used.

The step responses of the single-degree-of-freedom system with either the Dual Phase Advance or the PD controllers are plotted after evaluating and producing the closed loop transfer function.

The remaining M files evaluate the five-degree-of-freedom step responses for the continuous and discrete-time, they also evaluate the five percent over-shoot and under-shoot, and the settling-time.

DEFINITIONS OF VARIABLES		
nump	=	Single-Degree-of-Freedom power supply numerator.
denp	=	" " " " " " denominator.
nnum	=	" " " " plant numerator.
nden	=	" " " " plant denominator.
numpa	=	Phase Advanced Controller numerator.
denpa	=	" " " denominator.
num2pa	=	Dual Phase Advanced Controller numerator.
den2pa	=	" " " " denominator.
snum	=	Uncompensated system numerator.
sden	=	" " denominator.
cnum	=	Compensated system numerator.
cden	=	" " denominator.
clnum	=	Closed loop numerator.
clden	=	Closed loop denominator.
t	=	Time.
dt	=	Time increment.
time	=	Time vector.
zfreq	=	Zero frequency.
setime	=	Settling time.
cnt	=	Counter.
errup	=	The value of the error above zero frequency.
errdn	=	" " " " " below " " .

Table B.1 List of variables of the single degree-of-freedom M files.

Root Locus:

```
% Evaluating the system's and the
% controller's transfer functions.

snum = conv(nump,nnum)*.0126;     % Combining the plant and the power
sden = conv(denp,nden)           % supply transfer functions.
num2pa = conv(numpa, numpa);      % Creating Dual Phase Advance
den2pa = conv(denpa, denpa);      % controller transfer function.
cnum = conv(snum, num2pa);        % Creating the system's compensated
cden = conv(sden, den2pa);        % transfer function.
 vv=[x1,x2,y1,y2];               % Scaling the minimum and maximum
  axis(vv)                      % values of the axis.
  rlocus(cnum,cden)
 rlocfind(cnum,cden)
```

Dual Phase Advanced Step Responses:

```
snum = conv(nump,nnum)*.0126;
sden = conv(denp,nden);
num2pa = conv(numpa, numpa);
den2pa = conv(denpa, denpa);
gnum=conv(num2pa,snum);
gden=conv(den2pa,sden);
clnum=conv(snum,den2pa);          % Closed-loop transfer function numerator.
n=t/dt;
errup=1;
ymax=1e-15;
while ymax < errup,
 gain = gain+g1;
  if ymax < errup,
   ymax = 0;
  clden=gden+gnum*gain;
   zfreq = (clnum(1, 6) / clden(1, 6))    % Calculating the zero Frequency value.
    errdn = zfreq - .05 * zfreq;          % Error of five percent below zero frquency.
     errup = zfreq + .05 * zfreq;         %  "  "  "  "     above "    "  .
      gain
       y=step(clnum,clden,time);
      for cnt = 1 : n,
       if cnt > 1,
        if y(cnt) > y(cnt-1),       % Finding the maximum over-shoot.
          tmp=y(cnt);
        else
         end
       if tmp > ymax,
        ymax=tmp;
       else
```

```
        end
       else
        end

       if y(cnt) < errdn,              % Evaluating the settling time.
        setime1 = cnt*dt;
       elseif y(cnt) > errup,
        setime2 = cnt*dt;
       else
       end
      end
     if setime2 > setime1,
       setime1
       errdn
     else
       setime2
       errup
     end
    ymax
    pause
plot(y);title('Single-Degree-of-Freedom Step Response')
xlabel('Time = seconds x 100')
else
end
end
```

PD Step Response

```
snum = conv(nump,nnum)*.0126;
sden = conv(denp,nden);
gnum=conv(numpd,snum);
clnum=snum;
n=t/dt;
errup=1;
flag =0;
while flag ~= 1,
 gain = gain+g1;
  if ymax < errup,
    if ymax > (errup - errup * .01),   % With these statements, the over-shoot that falls
      flag = 1;                        % between four and five percent is getting evaluated.
    else
    end                               % The rest, the same explanation as above.
  else
  end
   ymax=0;
 clden=sden+gnum*gain;
  zfreq = (clnum(1,3)/clden(1,4))
```

```
      errdn = zfreq - .05 * zfreq;
       errup = zfreq + .05 * zfreq;
        gain
          y=step(clnum,clden,time);
         for cnt = 1 : n,
          if cnt > 1,
            if y(cnt) > y(cnt-1),
              tmp=y(cnt);
            else
             end
           if tmp > ymax,
            ymax=tmp;
           else
          end
         else
           end
         if y(cnt) < errdn,
          setime1 = cnt*dt;
         elseif y(cnt) > errup,
          setime2 = cnt*dt;
         else
         end
       end
      if setime2 > setime1,
        setime1
        errdn
      else
        setime2
        errup
      end
    pause
 plot(y);title('Single-Degree-of-Freedom Step Response')
  xlabel('Time = seconds x 100')
end
```

FIVE DEGREE OF FREEDOM SYSTEM

DEFINITIONS OF VARIABLES	
a,b,c,d	= Plant's state space matrices.
sa,sb,sc,sd	= System's state space matrices.
pa,pb,pc,pd	= Power supply state space matrices.
da,db,dc,dd	= Discrete time state space matrices.
fa,fb,fc,fd	= The feedback state space matrices of the entire system.
invl	= Inverse of the inductance matrix.
pbc	= The power supply B matrix multiplied by the decoupling matrix.
apa,apb,apc,apd	= The appended five dual phase advanced controllers state space matrices.
gain	= 5 x 5 gain matrix.
fivprovr	= Five percent over-shoot.
fivprund	= Five percent under-shoot.
tt	= Time vector.

Table B.2 List of variables of the five degree-of-freedom M files.

Continuas time step response:

```
pa = -eye(5) * fq * invl;
[sa,sb,sc,sd]=series(pa,pbc,pc,pd,a,b,c,d);
ap3=apc;
ap4=apd;
nn=t/dtt;
ymax=1e7;
fivprovr=0;
 while fivprovr < ymax,
  g1=g1+g2;
  gain(ui,ui)=g1;
    apc=gain*apc;
      apd=gain*apd;
        [fa,fb,fc,fd]=feedback(sa,sb,sc,sd,apa,apb,apc,apd);
          y=step(fa,fb,fc,fd,ui,tt);
            ymax=0;
     for ll = 1:nn+1,
       if uc == 8,
          y(ll,uc)=y(ll,uc)/.3048;    % .3048m is the model's length
        elseif uc == 3,               % 3 & 8 are the degree-of-freedom numbers
          y(ll,8)=y(ll,8)/.3048;
        end
         if ll > 1,
           if y(ll,uc) > y(ll-1,uc),
```

```
            str = y(ll,uc);
           else
           end
           if str > ymax,
            ymax = str;
           else
           end
            ys(ll)=y(ll,uc);
           if y(ll,uc) == ys(ll),
            tmp=y(ll,uc);
           else
           end
          else
          end
       end

       err=.05*tmp;
        fivprund=tmp-err;
        fivprovr=tmp+err;

      for lk=1:nn+1,
       if ys(lk) < fivprund,
        stime1 = lk*dtt;
       elseif ys(lk) < fivprovr,
        stime2 = lk*dtt;
       else
       end
      end
       if stime1 < stime2,
        setltime = stime1
       else
        setltime = stime2
       end
       g1
      ymax
      fivprovr
      apc=ap3;
    apd=ap4;
 end
   plot(y);title('Continuous-Time Step Response')
end
```

Discrete with time delay M file:

This M file converts the continuas closed loop system matrices to discrete with time delay system matrices, then, the step responses of those matrices is plotted. Pade command was used since it returns an nth order pade approximation to a time delay.

```
for lam=s1:s2:s3,
 ap3=gain*apc;
 ap4=gain*apd;
 nn=time/samp;
 [lma,lmb,lmc,lmd]=pade(lam,ord);                    % ord is the order system.
 [la,lb,lc,ld]=append(lma,lmb,lmc,lmd,lma,lmb,lmc,lmd);
  for i=1:3,
    [la,lb,lc,ld]=append(la,lb,lc,ld,lma,lmb,lmc,lmd);
  end
 [dsa,dsb,dsc,dsd]=series(apa,apb,ap3,ap4,la,lb,lc,ld);
 [fa,fb,fc,fd]=feedback(sa,sb,sc,sd,dsa,dsb,dsc,dsd);
[da,db,dc,dd]=c2dt(fa,fb,fc,samp,lam2);          % Samp is the sampling time.
sy=dstep(da,db,dc,dd,ui,nn);                      % lam is the delay time.

   for ll = 1:nn+1,
     if uc == 8,
       sy(ll,uc)=sy(ll,uc)/.3048;                  % .3048m is the model's length.
      elseif uc == 3,                             % 3 & 8 are the mode numbers.
       sy(ll,8)=sy(ll,8)/.3048;
      else
      end
   end
plot(sy),title('Discrete-Time Step Response')
xlabel('Number of points')                        % nn is the number of points.
ap3=0;                                          % t is the time vector with
ap4=0;                                          % interval = sampling time.
end
```

APPENDIX C

This program generates random numbers to be used as noise in order to test the behavior of the Dual Phase Advanced and PID controllers. This program which was written originally by W. A. Kilgore (Ref. 5) compares different controllers with Single-Degree-of-Freedom Feedback magnetic suspension system.

```
            CLS
            CLEAR
    DIM M(2000), GS(2000), XA(2000)
    COLOR 12
            PI = 3.14159
            N = 1000
            LOCATE 12, 22: PRINT "Generating random numbers (noise)"
            FOR I = 1 TO N
              M(I) = RND
                   SUM = SUM + RND
            NEXT I
              MN = SUM / N
            FOR L = 1 TO N
              SG = M(L) ^ 2 - MN ^ 2
              GS(L) = (1 / (2 * PI * SG)) * EXP(-(M(L) - MN) ^ 2 / 2 * SG)
            NEXT L

'OPEN "a:pid.mat" FOR OUTPUT AS #1
'Sampling Time
            T = .01
'The MSBS plant variables
            Kx = -1
            Kc = -.1
            Ki = .1
            M = 1
            R = 1
            L = .1
            C = 0
'The MSBS plant coefficients
            a0 = -Ki / M / L
            a1 = R / M / L + 2 / M / T
            a2 = 3 * R / M / L + 2 / M / T
            a3 = 3 * R / M / L - 2 / M / T
            a4 = R / M / L - 2 / M / T
```

```
                b0 = (2 / T) ^ 3 + (2 / T) ^ 2 * (R / L + C / M) + 2 / T * (C * R / M / L
 + Kx /           M - Ki * Kc / L / M) + R * Kx / L / M
                b1 = -3 * (2 / T) ^ 3 - (2 / T) ^ 2 * (R / L + C / M) + 2 / T * (C * R / M /
L + Kx           / M - Ki * Kc / L / M) + 3 * R * Kx / L / M
                b2 = 3 * (2 / T) ^ 3 - (2 / T) ^ 2 * (R / L + C / M) - 2 / T * (C * R / M / L
 + Kx            / M - Ki * Kc / L / M) + 3 * R * Kx / L / M
                b3 = -(2 / T) ^ 3 + (2 / T) ^ 2 * (R / L + C / M) - 2 / T * (C * R / M / L +
Kx /            M - Ki * Kc / L / M) + R * Kx / L / M
'Screen layout
                tmax = 10
                tmin = 0
                XMAX = 2
                xmin = 0
                SCREEN 9
                  COLOR 14, 3
                  'VIEW (30, 125)-(610, 320), 8   ' Original
                  VIEW (30, 105)-(610, 300), 8
                WINDOW (tmin - .01 * tmax, xmin - .02 * XMAX)-(tmax + .01 * tmax,
XMAX +                .02 * XMAX)
'Borders
                LINE (tmin, xmin)-(tmin, XMAX), 13
                LINE (tmin, xmin)-(tmax, xmin), 13
                LINE (tmin, XMAX)-(tmax, XMAX), 13
                LINE (tmax, xmix)-(tmax, XMAX), 13
'Horizontal lines
                LINE (tmin, .25 * XMAX)-(tmax, .25 * XMAX), 10, , &HFF00
                LINE (tmin, .5 * XMAX)-(tmax, .5 * XMAX), 10, , &HFF00
                LINE (tmin, .75 * XMAX)-(tmax, .75 * XMAX), 10, , &HFF00
'Vertical lines
                LINE (tmax * .1, xmin)-(tmax * .1, XMAX), 10, , &HFF00
                LINE (tmax * .2, xmin)-(tmax * .2, XMAX), 10, , &HFF00
                LINE (tmax * .3, xmin)-(tmax * .3, XMAX), 10, , &HFF00
                LINE (tmax * .4, xmin)-(tmax * .4, XMAX), 10, , &HFF00
                LINE (tmax * .5, xmin)-(tmax * .5, XMAX), 10, , &HFF00
                LINE (tmax * .6, xmin)-(tmax * .6, XMAX), 10, , &HFF00
                LINE (tmax * .7, xmin)-(tmax * .7, XMAX), 10, , &HFF00
                LINE (tmax * .8, xmin)-(tmax * .8, XMAX), 10, , &HFF00
                LINE (tmax * .9, xmin)-(tmax * .9, XMAX), 10, , &HFF00
'Label
                LOCATE 12, 2: PRINT "P"
                LOCATE 13, 2: PRINT "o"
                LOCATE 14, 2: PRINT "s"
                LOCATE 15, 2: PRINT "i"
                LOCATE 16, 2: PRINT "t"
                LOCATE 17, 2: PRINT "i"
                LOCATE 18, 2: PRINT "o"
                LOCATE 19, 2: PRINT "n"
                LOCATE 2, 30: PRINT "MSBS Simulation"
```

```
'Input step of position
    'ref = 1
            LOCATE 3, 2: PRINT TIME$
52    Total = Total + T
            'GOSUB 100  'DPA, Tustin's Method (Appendix B)    Feedback (Done)
            GOSUB 1100  'PID, Tustin's Method (Appendix B)    Feed forward (Done)
'Total Error Sum
'     SUError = ABS(Xp1 - X) / ref + SUError
'Max. Overshoot or undershoot and Peak Time for Position Input
            IF Total > 5 THEN 72
            IF X > MAXX THEN 61
            GOTO 63
61    IF MX1 = 0 THEN 62
            IF X < MX1 THEN 73        'MX1 AND MX11 ARE STORAGE POINTS'
62    MX1 = X
            IF MX11 > MX1 THEN 73
            MX11 = MX1
            MAXX = X
            PCNT = X - 1
            PTIME = Total
            GOTO 73
63    IF MX2 = 0 THEN 64
            IF X > MX2 THEN 65        'MX2 IS A STORAGE POINT
64    MX2 = X
            MXD1 = ABS(1 - MX2)         'MXD1 AND MXD2 ARE DISTANCES
            IF MXD2 > MXD1 THEN 65      'BETWEEN THE TWO PEAKS
            MXD2 = MXD1
            X1 = X
            TOT = Total
            GOTO 73
65    MAXX = X1
            PCNT = X1 - 1
            PTIME = TOT
72    IF Total < 5 THEN 73
            MAXX = PCNT
73

'Max. Overshoot and Peak Time for Force Input
            IF Total > 5 AND X > MAX2 THEN MAX2 = X
            IF X = MAX2 THEN PTIME2 = Total
'Rise Time
            IF X <= (.1 * ref) THEN RT1 = Total
            IF jj = 1 THEN GOTO 98
            IF X >= (.9 * ref) THEN jj = 1
            IF X >= (.9 * ref) AND jj = 1 THEN RT2 = Total
            RISE = RT2 - RT1
    '  LOCATE 6, 15: PRINT "Rise Time =": LOCATE 6, 27: PRINT USING "##.###";
RISE
```

```
98    ' LOCATE 9, 13: PRINT "Overshoot 1 =": LOCATE 9, 27: PRINT USING "##.###";
MAXX
      ' LOCATE 7, 13: PRINT "Peak Time 1 =": LOCATE 7, 27: PRINT USING "##.###";
PTIME
      ' LOCATE 7, 43: PRINT "Peak Time 2 =": LOCATE 7, 57: PRINT USING "##.###";
PTIME2
      ' LOCATE 5, 20: PRINT "Time =": LOCATE 5, 26: PRINT USING " ##.###"; Total
      ' LOCATE 5, 46: PRINT "Position =": LOCATE 5, 57: PRINT USING "##.###"; X
      ' LOCATE 9, 43: PRINT "Overshoot 2 =": LOCATE 9, 57: PRINT USING "##.###";
MAX2
'Position Input Settling Time
                p = .001
                IF jjj = 1 THEN GOTO 59
                IF (ABS(Xp1 - X) < p * X) AND (ABS(Xp2 - X) < p * X) AND (ABS(Xp3
- X) <          p * X) AND (ABS(Xp4 - X) < p * X) AND (ABS(Xp5 - X) < p * X) AND
(ABS(XP6 - X) <          p * X) AND (ABS(Xp7 - X) < p * X) AND (ABS(Xp8 - X) < p *
X) THEN SETTIME = Total
                IF SETTIME = Total THEN jjj = 1
      ' LOCATE 8, 9: PRINT "Settling Time 1 = ": LOCATE 8, 27: PRINT USING "##.###
";              SETTIME
59 'Force Input Settling Time
                pp = .0005
                IF jjjj = 1 THEN GOTO 70
                IF fd > 1 THEN GOTO 60 ELSE GOTO 70
60      IF ABS(X - ref) / ref < pp AND ABS(Xp1 - ref) / ref < pp AND ABS(Xp2 - ref) / ref
< pp              AND ABS(Xp3 - ref) / ref < pp AND ABS(Xp4 - ref) / ref < pp AND
ABS(Xp5 - ref) / ref            <pp AND ABS(XP6 - ref) / ref < pp AND ABS(Xp7 - ref) / ref
< pp AND
        ABS(Xp8 - ref) / ref < pp THEN SETTIME2 = Total
                IF SETTIME2 = Total AND Total > 6 THEN jjjj = 1
      ' LOCATE 8, 39: PRINT "Settling Time 2 =": LOCATE 8, 57: PRINT USING "##.###
";              SETTIME2
'Shift the variables back in time
70      fdp3 = fdp2
                fdp2 = fdp1
                fdp1 = fd
                Xp8 = Xp7
                Xp7 = XP6
                XP6 = Xp5
                Xp5 = Xp4
                Xp4 = Xp3
                Xp3 = Xp2
                Xp2 = Xp1
                Xp1 = X
                Ep3 = Ep2
                Ep2 = Ep1
                Ep1 = E
                Vp3 = Vp2
```

```
                Vp2 = Vp1
                Vp1 = V

        PSET (Total, X + 1), 12:
                COUNT = COUNT + 1
                LOCATE 23, 40: PRINT COUNT
'       PRINT #1, USING "###.#######"; X

 'Input step of force
     ' IF Total > 5 THEN fd = 10

        SUMX = SUMX + X
        XA(COUNT) = X
                IF Total > tmax AND Total < tmax + T THEN GOTO 80 ELSE GOTO 52
 80     LOCATE 24, 37: PRINT "Time"

     AVG = SUMX / COUNT

    FOR LK = 1 TO COUNT
     XTX = (XA(LK) - AVG) ^ 2
     SUMXTX = SUMXTX + XTX
    NEXT LK
  RMS = SQR(SUMXTX / COUNT)          '<------- The standard deviation

                LOCATE 6, 25: PRINT "The RMS value = "; USING "##.####"; RMS
       CLOSE #1
 88   END

          'Subrountines

 100 'Dual PA, Tustin's Method (Appendix B)
    'This controller is located in the feedback path
                IF first = 1 GOTO 110
                K = -2784
                LOCATE 3, 21: PRINT "Tustin's Method, Dual Phase Advance"
                LOCATE 4, 35: PRINT "K="; K
                gain = 1
                Kin = .5
                A = .01
                N = 10
                c0 = (T * T + 4 * N * A * T + 4 * N * N * A * A) / (T * T + 4 * A * T +
4 * A           * A)
                c1 = (2 * T * T - 8 * N * N * A * A) / (T * T + 4 * A * T + 4 * A * A)
                c2 = (T * T - 4 * N * A * T + 4 * N * N * A * A) / (T * T + 4 * A * T +
4 * A           * A)
                c3 = (2 * T * T - 8 * A * A) / (T * T + 4 * A * T + 4 * A * A)
                c4 = (T * T - 4 * A * T + 4 * A * A) / (T * T + 4 * A * T + 4 * A * A)
                d1 = Kin * T
```

```
110    CNT = CNT + 1
               E = ref * gain - G
               Etotal = E + Etotal
               Z = E + d1 * Etotal
               V = K * Z
               X = (a0 * (V + Vp1 + Vp2 + Vp3) + a1 * fd + a2 * fdp1 + a3 * fdp2 +
a4 * fdp3          - b1 * Xp1 - b2 * Xp2 - b3 * Xp3) / b0
               X = X + GS(CNT) * .0001
               G = c0 * X + c1 * Xp1 + c2 * Xp2 - c3 * Gp1 - c4 * Gp2
               Gp2 = Gp1
               Gp1 = G
               first = 1
               RETURN


1100 'PID Tustin's Method, (Appendix B)
   'This controller is located in the feed forward path.
               IF first = 1 GOTO 1110
               K = -396
               LOCATE 3, 28: PRINT "PID Tustin's Method"
               LOCATE 4, 35: PRINT "K="; K
               gain = 1
               Kp = 1
               Kd = .4
               Kin = .5
               c1 = Kp + 2 * Kd / T + T * Kin / 2
               c2 = T * Kin - 4 * Kd / T
               c3 = T * Kin / 2 + 2 * Kd / T - Kp
1110  CNT = CNT + 1
               E = ref * gain - G
               Z = c1 * E + c2 * Ep1 + c3 * Ep2 + Zp2
               V = K * Z
               X = (a0 * (V + Vp1 + Vp2 + Vp3) + a1 * fd + a2 * fdp1 + a3 * fdp2 +
a4 * fdp3          - b1 * Xp1 - b2 * Xp2 - b3 * Xp3) / b0
               X = X + GS(CNT) * .0001
   G = X
               Zp2 = Zp1
               Zp1 = Z
               first = 1
               RETURN
```